

Weakly turbulent laws of wind-wave growth

SERGEI I. BADULIN¹, ALEXANDER V. BABANIN²,
VLADIMIR E. ZAKHAROV^{3,4,5} AND DONALD RESIO⁶

¹P. P. Shirshov Institute of Oceanology of Russian Academy of Sciences Moscow, Russia

²Swinburne University of Technology, Melbourne, Australia

³Waves and Solitons LLC, Phoenix, Arizona, USA

⁴P. N. Lebedev Physical Institute of Russian Academy of Sciences, Moscow, Russia

⁵University of Arizona, Tuscon, USA

⁶Waterways Experiment Station, USA, Vicksburg, Massachusetts, USA

(Received 14 June 2006 and in revised form 11 July 2007)

The theory of weak turbulence developed for wind-driven waves in theoretical works and in recent extensive numerical studies concludes that non-dimensional features of self-similar wave growth (i.e. wave energy and characteristic frequency) have to be scaled by internal wave-field properties (fluxes of energy, momentum or wave action) rather than by external attributes (e.g. wind speed) which have been widely adopted since the 1960s. Based on the hypothesis of dominant nonlinear transfer, an asymptotic weakly turbulent relation for the total energy ε and a characteristic wave frequency ω_* was derived

$$\frac{\varepsilon \omega_*^4}{g^2} = \alpha_{ss} \left(\frac{\omega_*^3 d\varepsilon/dt}{g^2} \right)^{1/3}.$$

The self-similarity parameter α_{ss} was found in the numerical duration-limited experiments and was shown to be naturally varying in a relatively narrow range, being dependent on the energy growth rate only.

In this work, the analytical and numerical conclusions are further verified by means of known field dependencies for wave energy growth and peak frequency downshift. A comprehensive set of more than 20 such dependencies, obtained over almost 50 years of field observations, is analysed. The estimates give α_{ss} very close to the numerical values. They demonstrate that the weakly turbulent law has a general value and describes the wave evolution well, apart from the earliest and full wave development stages when nonlinear transfer competes with wave input and dissipation.

1. Introduction

Over some 50 years, the wind-generated ocean waves have been extensively approached by experimental, numerical and theoretical means. All these approaches are united by the concept of spectral balance. Hasselmann (1962, 1963*a*, *b*) derived ‘from first principles’ the conservative kinetic equation describing this balance in terms of spectral density of wave action $N(\mathbf{k}, t)$ for spatially homogeneous ocean:

$$\frac{\partial N(\mathbf{k}, t)}{\partial t} = S_{nl}[N(\mathbf{k})]. \quad (1.1)$$

The nonlinear term S_{nl} on the right-hand side of (1.1) is the so-called collision integral that describes the effect of four-wave resonant interactions. The explicit form of the term is known and can be found in a number of papers (see e.g. Hasselmann 1962; Webb 1978; Zakharov 1999; Lavrenov 2003). Generalization of (1.1) for the case of non-homogeneous ocean,

$$\frac{\partial N_{\mathbf{k}}}{\partial t} + \nabla_{\mathbf{k}} \omega_{\mathbf{k}} \nabla_r N_{\mathbf{k}} = S_{nl}[N(\mathbf{k})], \quad (1.2)$$

is trivial, but it implies that inhomogeneity and non-stationarity are weak: the corresponding terms should have the same weakly nonlinear scaling as the collision term. In this case, S_{nl} depends on ‘local and instantaneous’ wave spectra only, and does not depend on time and coordinates explicitly.

The kinetic equations (1.1), (1.2) in their original forms are not complete because they do not comprise effects of wind-wave interactions and dissipation. Corresponding terms of wave input S_{in} and dissipation S_{diss} which describe a great number of physical effects associated with wind-wave development are incorporated into the kinetic Hasselmann equation phenomenologically

$$\frac{\partial N_{\mathbf{k}}}{\partial t} + \nabla_{\mathbf{k}} \omega_{\mathbf{k}} \nabla_r N_{\mathbf{k}} = S_{nl}[N(\mathbf{k})] + S_{in} + S_{diss}. \quad (1.3)$$

Despite the painstaking efforts of both experimentalists and theoreticians, the new constituents of wind-wave balance in the ‘full’ kinetic equation (1.2) are not well-known: discrepancies between different estimates can exceed one order in magnitude (see §3 and figure 1 in Badulin *et al.* 2005*b*). Moreover, mathematical forms of these terms are unknown: experimental parameterizations, generally, use quasi-linear functions of spectral density $N(\mathbf{k})$. The uncertainty in non-conservative terms S_{in} , S_{diss} gives wave modellers a free hand to tune the magnitudes of these terms in wave-forecasting models. This does not provide any understanding of physical laws governing growth of wind-driven waves.

An important hypothesis has been formulated by Zakharov (1966) (see also Zakharov & Zaslavsky 1982): for developing sea nonlinear transfer the term S_{nl} is a leading term if compared with wave input S_{in} and dissipation S_{diss} . This leadership has certain constraints. It is not, obviously, the case for matured sea (old wind waves) when all the constituents contribute equally to the wind-wave balance. An opposite case of very young waves (very short durations and fetches) falls beyond the scaling of the kinetic equation itself (see for details Hasselmann 1962; Zakharov 1999). In particular, wind-wave tanks appear to be inadequate tools for modelling statistical properties of real wind seas: the largest installations provide first hundreds of wave periods, at best, while one- to two-order larger scales are required for the kinetic equation to be valid. Additionally, waves in these tanks are quasi-unidirectional, i.e. nonlinear resonances in these tanks are corrupted by boundaries unpredictably.

Fortunately, the range of ‘adult’ growing wind-driven seas governed by leading nonlinear transfer is quite wide. This conclusion has been supported by a numerical study (Badulin *et al.* 2005*b*) and an experimental justification has been presented by Zakharov (2005*b*).

The purpose of this paper is to verify the hypothesis of leading nonlinear transfer for growing wind-driven seas in terms of dependencies of wave growth on duration and fetch. We use results of numerical studies of the duration-limited growth (Badulin *et al.* 2005*b*) and known fetch-limited experimental dependencies obtained by different authors.

A key consequence of dominating nonlinearity in the kinetic equation (1.3) is a strong tendency of its solutions towards self-similar behaviour. These self-similar solutions are approximations valid for fetch-limited (stationary) or duration-limited (spatially homogeneous) set-ups. As a result, total wave energy and characteristic frequency (mean or spectral peak one) for these self-similar solutions evolve as power functions of fetch (time)

$$\tilde{\varepsilon}(\tau) = \tilde{\varepsilon}_0 \tau^{p_\tau}, \quad \tilde{\omega}_*(\tau) = \tilde{\omega}_0 \tau^{-q_\tau}, \quad (1.4)$$

$$\tilde{\varepsilon}(\chi) = \tilde{\varepsilon}_0 \chi^{p_\chi}, \quad \tilde{\omega}_*(\chi) = \tilde{\omega}_0 \chi^{-q_\chi}. \quad (1.5)$$

Here τ , χ , $\tilde{\varepsilon}$, $\tilde{\omega}_*$ are non-dimensional time, fetch, total energy and characteristic frequency and $\tilde{\varepsilon}_0$, $\tilde{\omega}_0$ are corresponding scales of energy and frequency. The scaling of dependencies (1.4), (1.5) is a delicate matter that will be detailed below.

These particular self-similar solutions (in duration- and fetch-limited cases), in fact, represent two-parametric families of solutions. As a result, in dependencies (1.4), (1.5) there are links between exponents and pre-exponents of energy growth and frequency downshift. Exponents p_τ , q_τ (p_χ , q_χ) are related to each other by a linear dependence: steeper energy growth gives faster downshift (characteristic frequency relaxation). Interrelation of pre-exponents $\tilde{\varepsilon}_0$, $\tilde{\omega}_0$ has a more complicated form, but it reflects the basic feature of the conservative kinetic equation (1.2) – the rigid link between spectral fluxes and spectra themselves. Thus, it provides a bridge to the classic results of theory of weak turbulence, the stationary Kolmogorov–Zakharov (KZ) flux solutions (Zakharov & Filonenko 1966; Zakharov & Zaslavsky 1982).

Power-law dependencies (1.4), (1.5) are well-known to everybody who deals with wind-wave studies: results of measurements of wave growth are usually expressed by power-law fits (1.4), (1.5). Following Kitaigorodskii (1962), scaling of the dependencies is defined in a standard way as follows

$$\tilde{\omega} = \omega U_h / g, \quad \tilde{\varepsilon} = \varepsilon g^2 / U_h^4, \quad \chi = gx / U_h^2, \quad \tau = gt / U_h, \quad (1.6)$$

where U_h is wind speed at a reference height (or its substitute – friction velocity u^*) and g is acceleration due to gravity. Pre-exponents and exponents vary broadly in different experiments. For fetch-limited dependencies (1.5), we have (see dependencies collected in Davidan 1995; Babanin & Soloviev 1998a; Young 1999)

$$0.7 < p_\chi < 1.1, \quad 0.23 < q_\chi < 0.33, \quad (1.7)$$

$$0.68 \times 10^{-7} < \tilde{\varepsilon}_0 < 18.9 \times 10^{-7}, \quad 10.4 < \tilde{\omega}_0 < 22.7. \quad (1.8)$$

The great scatter of fitting parameters (e.g. more than an order of magnitude for total energy) has no explanation within the present vision (mostly experimental) of wave growth. As Donelan *et al.* (1992), p. 477) pointed out:

‘Perhaps it is time to abandon the idea that a universal power law for non-dimensional fetch-limited growth rate is anything more than an idealization.’

In the meantime, a number of workers attempted to reconcile results of different experiments and to propose a universal dependence (see Wen *et al.* 1993; Hwang 2006). It is in sharp contrast to our theoretical results: differences in self-similar solutions that correspond to power-law dependencies (1.4), (1.5) are legitimate and comprise a family of wave growth dependencies where exponents and pre-exponents can vary in wide ranges. Thus, there is no universality in the sense of fixed exponents and pre-exponents of wave growth, but there is a universality of interrelations of these exponents and pre-exponents. These interrelations can be expressed in compact

form as a self-similar law of wind-wave growth,

$$\frac{\varepsilon \omega_p^4}{g^2} = \alpha_{ss} \left(\frac{\omega_*^3 d\varepsilon/dt}{g^2} \right)^{1/3}, \quad (1.9)$$

that links total energy, characteristic frequency and net total wave input. We use the full derivative d/dt to stress the general nature of the law. α_{ss} is a self-similarity parameter that may depend on the scenario (duration- or fetch-limited) and rate of wave growth (exponents p_τ, p_χ). We specify α_{ss} below and show that these dependencies can be considered as relatively weak for typical wind-sea conditions.

The self-similarity of wind-driven seas expressed by (1.9) is just a special case, a visible part of the leading nonlinear transfer, i.e. of the general weakly turbulent mechanisms that control wind-wave growth. As is often the case in physics, this special case appears to be extremely robust. This is why the relationship (1.9) can be considered as a general law applicable to the wave growth, regardless of a particular dependence of wind forcing on time (fetch). This law simply reflects an existing link between total energy and total wave input associated with inverse cascade mechanism. Hereinafter, we use total wave input to mean the difference between the wind input and wave energy dissipation, accumulated by the waves. It gives grounds to present the asymptotic law (1.9) as the weakly turbulent law of wave growth.

The asymptotic self-similar relationship (1.9) is in contrast with a traditional approach to wave growth. Starting with Kitaigorodskii (1962) (and, in fact, much earlier), wave growth is scaled by wind speed (see (1.6)) and by the corresponding non-dimensional parameter of wave age U_h/C_p (or u_*/C_p). Such scaling, in fact, implies a universality of wind-wave interaction which is not the case. Significant scatter of wave growth dependencies around a representative one is generally attributed to deviations from ‘standard’ conditions of wave development owing to, say, gustiness (Abdalla & Cavaleri 2002), stability of atmosphere, presence of swell, fine-scale inhomogeneity of wave skewness and asymmetry that can all affect the wave growth rate, sometimes by a factor of 2–3 (e.g. Donelan *et al.* 2005). All these factors usually accompany wave growth which makes the corresponding wave growth description ‘reactive’ with respect to the wind speed scaling that is not able to account for all details of wind-wave interaction. On the contrary, our formulation in terms of net total wave input has a chance to be proactive, i.e. such scaling is able to document wave growth in a wide range of wind-wave conditions.

In §2, we provide physical and mathematical background for weakly turbulent self-similar solutions of the Hasselmann equation (Hasselmann 1962). The experimental concept of similarity analysis (Kitaigorodskii 1962) and experimental results themselves (Hasselmann *et al.* 1973) contain important physical hints towards the self-similarity. We detail the idea of the split energy balance for growing wind-driven seas and present simple expressions for the exponents and pre-exponents of wind-wave growth in duration- and fetch-limited cases.

In §3, the self-similar law (1.9) of wave growth is verified for duration-limited numerical experiments. The self-similarity parameter α_{ss} of (1.9) is estimated numerically for a wide range of physical conditions.

In §4, the theoretical relationships for exponents and pre-exponents of power-law dependencies (1.4), (1.5) are verified by means of fetch-limited field measurements. Zakharov (2005*b*) has demonstrated that exponents of fetch-limited growth in (1.5) satisfy theoretical relations for approximate self-similar solutions of the Hasselmann equation well. We extend this analysis to a larger set of fetch-limited sea experiments.

The self-similarity parameter α_{ss} , for the field experiments, appears to be close to numerical estimates of §3, i.e. validity of weakly turbulent wave growth law (1.9) does not depend on experimental set-up (duration- or fetch-limited). This validates the physical relevance of our approach: the wave energy content is controlled by non-stationary (duration-limited case) and non-homogeneous (fetch-limited case) parts of the full derivative of total energy $d\langle\varepsilon\rangle/dt$ (total flux) in a similar way.

Discussion and conclusions are given in §§5 and 6. In particular, the experimentally discovered Toba's law is examined and found to be a particular case of the presented weakly turbulent law when energy input is constant throughout the wave development.

2. Self-similar solutions and the split balance of growing wind waves

To begin with, we would like to repeat a key message of §1:

Difficulties of the studies of the 'full' Hasselmann equation (1.3) result, first of all, from our poor knowledge of external forcing terms, wind input and dissipation.

At first glance, hypothesis of the leading role of the nonlinear transfer term S_{nl} resolves this problem by making possible the asymptotic approach. In the first-order approximation, we have the conservative Hasselmann equation (1.2) with no external forcing, while a higher-order approximation takes into account formally small wind input and dissipation. The idea looks attractive and allows us to avoid a number of stumbling questions on properties of unknown terms of the external forcing. Some general features of this forcing turn out to be sufficient to define the wave development. We should stress that the asymptotic approach does not mean that we disregard wind input and dissipation, we just put them into their proper place. The asymptotic scheme has been realized in a number of ways (see Zakharov & Zaslavsky 1983; Zakharov 2005*b*; Badulin *et al.* 2006) and taken its form of *split balance model* in Badulin *et al.* (2005*a, b*, 2006).

The asymptotic procedure, when input and dissipation terms S_{in} and S_{diss} are assumed to be formally small, leads to the conservative kinetic equation (1.2) in the lowest order. This equation looks similar to the Boltzmann equation for gasdynamics. However, there is a dramatic difference between these equations. The Boltzmann equation is complete and self-sustained. It has a unique solution at any initial data. Temporal evolution of this solution preserves energy, momentum and total action (number of particles). On the contrary, the Hasselmann kinetic equation (1.2) preserves energy and momentum only formally (Pushkarev, Resio & Zakharov 2003, 2004). Because of the presence of the Kolmogorov-type cascades, the energy and the momentum can 'leak' at a high-wavenumber region. This region can also work as a source of wave action, energy and momentum. Thus, the conservative equation (1.2) is not 'complete'. It describes an 'open system' and has to be closed with a 'boundary condition', suppose, in the form of wave action flux at high frequencies. The full equation (1.3), with a sufficiently large dissipation term at high frequencies, appears to be well-posed. The former constants of motion cease to be constants, but the balance equation for total wave action remains valid and can be used to close the approximation procedure. The closure equation,

$$\left\langle \frac{\partial N_k}{\partial t} + \nabla_k \omega_k \nabla_r N_k \right\rangle = \langle S_f \rangle, \quad (2.1)$$

allows us to advance both in mathematics and in the physics of wave growth. The system of two equations, conservative Hasselmann equation (1.2) and 'boundary' total

balance condition (2.1), turns out to be much simpler for analytical studies. Unknown details of wave forcing S_f appear to be of no importance within the asymptotic approach, they are replaced by total forcing $\langle S_f \rangle$ which is readily observable in field experiments.

Homogeneity properties of collision integral S_{nl} for deep-water waves

$$S_{nl} [vN(\kappa\mathbf{k})] = v^3 \kappa^{19/2} S_{nl} [N(\mathbf{k})] \quad (2.2)$$

give additional help to advance the study (v, κ are arbitrary positive multipliers). Self-similar solutions can now be obtained in an explicit form for two important cases of homogeneous growing wave field (duration-limited case) and stationary spatial growth (fetch-limited case). Having the conservative kinetic equation (1.2) as a part of the asymptotic split balance model, we can generalize the classic Kolmogorov–Zakharov solutions (Zakharov & Filonenko 1966; Zakharov & Zaslavsky 1982; Zakharov, Falkovich & Lvov 1992) for the case of growing wind sea and arrive on time-(fetch-) independent Kolmogorov–Zakharov relationships between wave energy and total wave input.

2.1. Self-similar solutions for duration-limited case

For the deep water case, there is no specific scaling and non-dimensional variables can be introduced in an arbitrary way

$$t = \tau/\omega_0, \quad \mathbf{k} = k_0\boldsymbol{\kappa}; \quad \tilde{\omega} = \omega_0\Omega, \quad \Omega = \sqrt{\kappa}, \quad \omega_0 = \sqrt{gk_0}. \quad (2.3)$$

Non-dimensional wave action \tilde{n} takes the form

$$N(\mathbf{k}) = \frac{g^4}{\omega_0^9} \tilde{n}(\boldsymbol{\kappa}).$$

Correspondingly,

$$N(\omega, \theta) = \frac{g^2}{\omega_0^6} \tilde{n}(\Omega), \quad E(\omega, \theta) = \frac{g^2}{\omega_0^5} \tilde{\varepsilon}(\Omega, \theta). \quad (2.4)$$

The split balance model (1.1), (2.1) has self-similar solutions

$$\tilde{n}(\boldsymbol{\kappa}, \tau) = a_\tau \tau^{\alpha_\tau} \Phi_{\beta_\tau}(\boldsymbol{\xi}), \quad (2.5)$$

where

$$\boldsymbol{\xi} = b_\tau \boldsymbol{\kappa} \tau^{\beta_\tau} \quad (2.6)$$

and relationships

$$\alpha_\tau = (19\beta_\tau - 2)/4, \quad a_\tau = b_\tau^{19/4} \quad (2.7)$$

are determined by properties of the homogeneity of the collision integral S_{nl} (2.2). The solution magnitudes can grow ($\alpha_\tau > 0$) while characteristic frequency (wavenumber) decreases with time ($\beta_\tau > 0$). These solutions can be related with the well-known phenomenon of downshifting of wind-wave spectra. Solution (2.5) is consistent with power-law growth of total wave action (energy or momentum). Imposing the second equation of the split balance model (2.1), we can specify parameter r_τ of the family of self-similar solutions – the exponent of total wave action growth

$$N_{tot} \sim \tau^{r_\tau}, \quad r_\tau = \alpha_\tau - 2\beta_\tau = (11\beta_\tau - 2)/4 = (11\alpha_\tau - 4)/19. \quad (2.8)$$

Similarly, for exponents of total energy and momentum, we have

$$E_{tot} \sim \tau^{p_\tau}, \quad p_\tau = \alpha_\tau - 5\beta_\tau/2 = (9r_\tau - 1)/11, \quad (2.9a)$$

$$M_{tot} \sim \tau^{m_\tau}, \quad m_\tau = \alpha_\tau - 3\beta_\tau = (7r_\tau - 2)/11. \quad (2.9b)$$

The following relationship between exponent of energy growth p_τ and exponent of downshift q_τ is of key interest for further discussion

$$p_\tau = \frac{9q_\tau - 1}{2}. \quad (2.10)$$

The shape function $\Phi_{\beta_\tau}(\xi)$ in (2.5) obeys the integro-differential equation

$$\begin{aligned} & [\alpha_\tau \Phi_{\beta_\tau} + \beta_\tau \xi \nabla_\xi \Phi_{\beta_\tau}] \\ &= 16\pi^5 \int d\xi_1 d\xi_2 d\xi_3 |\tilde{T}_{\xi_1, \xi_2, \xi_3}|^2 \delta(\xi + \xi_1 - \xi_2 - \xi_3) \delta(\sqrt{|\xi|} + \sqrt{|\xi_1|} - \sqrt{|\xi_2|} - \sqrt{|\xi_3|}) \\ & \times [\Phi_{\beta_\tau}(\xi_1) \Phi_{\beta_\tau}(\xi_2) \Phi_{\beta_\tau}(\xi_3) + \Phi_{\beta_\tau}(\xi) \Phi_{\beta_\tau}(\xi_2) \Phi_{\beta_\tau}(\xi_3) - \Phi_{\beta_\tau}(\xi) \Phi_{\beta_\tau}(\xi_1) \Phi_{\beta_\tau}(\xi_2) \\ & - \Phi_{\beta_\tau}(\xi) \Phi_{\beta_\tau}(\xi_1) \Phi_{\beta_\tau}(\xi_3)]. \end{aligned} \quad (2.11)$$

Properties of solutions for (2.11) have not been studied yet. Numerical study (Badulin *et al.* 2005b) of the full kinetic equation (1.3) shows that a strong tendency to the corresponding approximate solutions does exist, at least for ‘acceptable’ parameters of spectral growth (see §3 in Badulin *et al.* 2005b). The range of the parameters can be specified as the condition that external forcing (term S_f) does not grow infinitely and thus does not become a leading term in the right-hand side of (2.1) at long time. Thus, we can associate the ‘growing wind sea’ as growth that corresponds to these acceptable growth rates

$$\alpha_\tau > 1, \quad r_\tau > 7/19, \quad p_\tau > 4/19, \quad q_\tau > 3/19, \quad m_\tau > 1/19. \quad (2.12)$$

Note that all the exponents r_τ , p_τ , m_τ and the downshift exponent q_τ are positive for the acceptable wind-wave growth (2.12).

2.1.1. Self-similarity of spectral fluxes

Self-similarity of asymptotic solutions (2.5) implies self-similarity of corresponding spectral fluxes. This allows us to obtain remarkable expressions for non-dimensional fluxes in terms of the shape function $\Phi_{\beta_\tau}(\xi)$

$$\begin{aligned} \lim_{\tau \rightarrow \infty} \frac{\tilde{Q}(\tilde{\Omega}, \tau)}{a_\tau^{11/19} \tau^{s_q}} &= \tilde{Q}_{\beta_\tau}(\xi) = \int_{-\pi}^{\pi} \int_0^{|\xi|} \left(\beta_\tau |\xi|^2 \frac{\partial \Phi_{\beta_\tau}}{\partial |\xi|} + \alpha_\tau |\xi| \Phi_{\beta_\tau} \right) d|\xi| d\theta \\ &= \left[\int_{-\pi}^{\pi} \beta_\tau |\xi|^2 \Phi_{\beta_\tau} d\theta \Big|_0^{|\xi|} + r_\tau \int_{-\pi}^{\pi} \int_0^{|\xi|} |\xi| \Phi_{\beta_\tau} d|\xi| d\theta \right], \end{aligned} \quad (2.13)$$

$$\begin{aligned} \lim_{\tau \rightarrow \infty} \frac{\tilde{P}(\tilde{\Omega}, \tau)}{a_\tau^{9/19} \tau^{s_p}} &= \tilde{P}_{\beta_\tau}(\xi) = - \int_{-\pi}^{\pi} \int_0^{|\xi|} \left(\beta_\tau |\xi|^{5/2} \frac{\partial \Phi_{\beta_\tau}}{\partial |\xi|} + \alpha_\tau |\xi|^{3/2} \Phi_{\beta_\tau} \right) d|\xi| d\theta \\ &= - \left[\int_{-\pi}^{\pi} \beta_\tau |\xi|^{5/2} \Phi_{\beta_\tau}(\xi) d\theta \Big|_0^{|\xi|} + p_\tau \int_{-\pi}^{\pi} \int_0^{|\xi|} |\xi|^{3/2} \Phi_{\beta_\tau} d|\xi| d\theta \right], \end{aligned} \quad (2.14)$$

$$\begin{aligned} \lim_{\tau \rightarrow \infty} \frac{\tilde{K}(\tilde{\Omega}, \tau)}{a_\tau^{7/19} \tau^{s_m}} &= \tilde{K}_{\beta_\tau}(\xi) = - \int_{-\pi}^{\pi} \int_0^{|\xi|} \left(\beta_\tau |\xi|^3 \frac{\partial \Phi_{\beta_\tau}}{\partial |\xi|} + \alpha_\tau |\xi|^2 \Phi_{\beta_\tau} \right) d|\xi| d\theta \\ &= - \left[\int_{-\pi}^{\pi} \beta_\tau |\xi|^3 \Phi_{\beta_\tau}(\xi) d\theta \Big|_0^{|\xi|} + m_\tau \int_{-\pi}^{\pi} \int_0^{|\xi|} |\xi|^2 \Phi_{\beta_\tau} d|\xi| d\theta \right] \end{aligned} \quad (2.15)$$

where exponents of time dependencies are

$$s_q = r_\tau - 1, \quad s_p = p_\tau - 1, \quad s_m = m_\tau - 1.$$

The result of the integration is of fundamental interest: for positive exponents of wave action growth r_τ and energy growth p_τ , signs of fluxes Q and P are fixed and correspond to an inverse cascade regime, i.e. $Q > 0$, $P < 0$. The momentum flux is negative (again an inverse cascade) for the acceptable rates (2.12). Note that small rates $r_\tau < 7/19$ are of little interest for our analysis because the smallness of external forcing S_f as compared with collision integral S_{nl} is questionable in this case (see (2.12)).

The case of swell is of special interest. Parameter p_τ is negative for swell and both types of cascade co-exist for wave energy and momentum: an inverse cascade in a low-frequency band (small $|\xi|$) and a leakage of energy and momentum (a direct cascade) to high frequencies.

The ‘boundary condition’ (2.1) of the split balance model can be rewritten in terms of spectral fluxes at infinitely high frequency (total wave input or total flux). For total energy we have

$$\left\langle \frac{\partial E_k}{\partial t} \right\rangle = - \lim_{\omega \rightarrow \infty} P(\omega, t) = \Pi(t). \quad (2.16)$$

2.1.2. Spectra vs. spectral fluxes

Having self-similar dependencies for solutions (2.5) and fluxes (2.13)–(2.15), we can easily construct time-independent quantities which are direct analogues of the classic Kolmogorov constants (Zakharov 1966, 1999). In terms of frequency spectra, it takes time-independent ratios

$$C_q^{(\beta_\tau)}(\xi) = \lim_{t \rightarrow \infty} \frac{E(\omega, \theta, t) \omega^{11/3} g^{4/3}}{Q(\omega, t)^{1/3}} = \frac{\Phi_{\beta_\tau}(\xi) |\xi|^{11/3}}{\tilde{Q}(\xi)^{1/3}}, \quad (2.17a)$$

$$C_p^{(\beta_\tau)}(\xi) = \lim_{t \rightarrow \infty} \frac{E(\omega, \theta, t) \omega^4 g^{4/3}}{P(\omega, t)^{1/3}} = \frac{\Phi_{\beta_\tau}(\xi) |\xi|^4}{|\tilde{P}(\xi)|^{1/3}}, \quad (2.17b)$$

$$C_m^{(\beta_\tau)}(\xi) = \lim_{t \rightarrow \infty} \frac{E(\omega, \theta, t) \omega^{13/3} g^{4/3}}{K(\omega, t)^{1/3}} = \frac{\Phi_{\beta_\tau}(\xi) \xi^{25/6}}{|\tilde{K}(\xi)|^{1/3}}. \quad (2.17c)$$

Values $C_q(\xi)$, $C_p(\xi)$, $C_m(\xi)$ are direct generalizations of the Kolmogorov constants (Zakharov & Zaslavsky 1982; Zakharov *et al.* 1992). They depend on the self-similarity argument ξ which is proportional to non-dimensional wavenumber, and on the self-similarity index r_τ (or β_τ). Thus, self-similar solutions (2.5) can be rewritten in time-independent form in terms of the Kolmogorov relations (2.17). Such reformulation looks speculative as long as the properties of functions of self-similar variable ξ in (2.17) are not specified. It has been shown in numerical studies (Badulin *et al.* 2005b) that spectral shapes $\Phi_{\beta_\tau}(\xi)$ and self-similar shapes of spectral fluxes $\tilde{Q}(\xi)$, $\tilde{P}(\xi)$, $\tilde{K}(\xi)$ manifest certain properties of quasi-universality, i.e. they depend slightly on the self-similarity index r_τ (or β_τ).

Figure 1 shows solutions of the Hasselmann equation, compensated spectra, wave action flux and the corresponding KZ function C_q plotted *vs.* the self-similar variable – non-dimensional wavenumber ξ . The plots are given for different times and thus demonstrate the asymptotic tendency of the spectra and spectral fluxes to the self-similar behaviour. Function $C_q(\xi)$ shows the most interesting feature of the behaviour: it forms a plateau for non-dimensional wavenumbers $|k/k_p| > 2.5$ ($\omega/\omega_p \gtrsim 1.5$). The ordinate of the plateau is close to the classic KZ constant of the inverse cascade obtained numerically (Lavrenov, Resio & Zakharov 2002; Pushkarev *et al.* 2003) and analytically (Geogjaev & Zakharov 2007). It should be stressed that the asymptotic

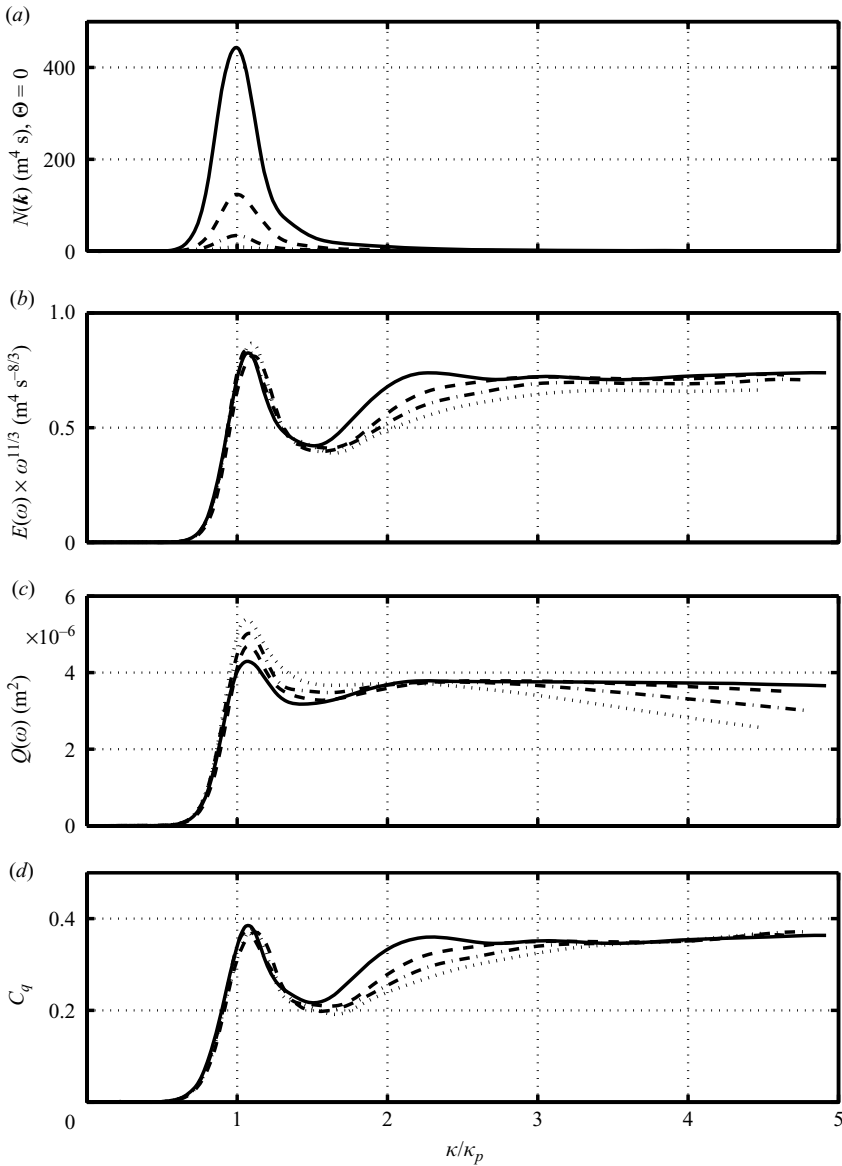


FIGURE 1. (a) Down-wind solution $N(\mathbf{k})$, (b) compensated frequency spectra of energy $E(\omega)\omega^{11/3}$, (c) wave action flux Q and (d) the resulting estimate of the Kolmogorov ratio C_q for solutions of the Hasselmann equation (1.3) at different times. Wave input by Hsiao & Shemdin (1983), wind speed 10 m s^{-1} , time of 4 (dotted), 8 (dash-dot), 16 (dashed), 32 h (solid line).

ratios of spectra and spectral fluxes (2.17) depend very slightly on wind input: different parameterizations of wind input were used by Badulin *et al.* (2005*b*) to show validity of the asymptotic interrelation of wave spectra and spectral fluxes. For energy spectra, it takes the following form

$$\lim_{t \rightarrow \infty} \frac{E(\omega, \theta, t)\omega^4}{g^2} = C_p^{(\beta;)}(\omega/\omega_p, \theta) \lim_{t \rightarrow \infty} \left(\frac{|P(\omega, t)|}{g^2} \right)^{1/3}. \quad (2.18)$$

Self-similarity of solutions (2.5) allows a number of different expressions for the relation of wave spectra to spectral fluxes, the most handy one can be proposed in terms of total energy ε and total wave input $\Pi(t)$ or total energy income $\partial\varepsilon/\partial t$ (see (2.18)). In non-dimensional form, the limit of (2.18) at $\omega \rightarrow \infty$ gives

$$\tilde{\varepsilon}\tilde{\omega}_*^4 = \alpha_{ss}^{(d)}(\tilde{\omega}_*^3\tilde{\Pi}(\tau))^{1/3} \tag{2.19}$$

or with (2.1)

$$\tilde{\varepsilon}\tilde{\omega}_*^4 = \alpha_{ss}^{(d)}\left(\tilde{\omega}_*^3\frac{\partial\tilde{\varepsilon}}{\partial\tau}\right)^{1/3}. \tag{2.20}$$

We use superscript (d) to stress that the dependence is derived for the particular case of duration-limited growth. For dimensional total energy and total wave input we obtain

$$\frac{\varepsilon\omega_*^4}{g^2} = \alpha_{ss}^{(d)}\left(\frac{\omega_*^3\Pi(t)}{g^2}\right)^{1/3} = \alpha_{ss}^{(d)}\left(\frac{\partial\varepsilon}{\partial t}\frac{\omega_*^3}{g^2}\right)^{1/3}. \tag{2.21}$$

Relationships (2.19)–(2.21) are fairly consistent with the split balance model, i.e. they operate with the same physical properties: characteristic frequency ω_* as a scale of conservative kinetic equation (1.1) and total wave input as a scale of the closure (boundary) condition (2.1), (2.16).

For total energy of self-similar solutions (2.5), we have

$$\tilde{\varepsilon} = \int \tilde{\Omega}(\kappa)\tilde{n}(\kappa) d\kappa = a_\tau^{9/19}\tau^{p_\tau} A_{\beta_\tau}, \quad A_{\beta_\tau} = \int |\xi|^{1/2}\Phi_{\beta_\tau}(\xi) d\xi. \tag{2.22}$$

Characteristic frequency $\tilde{\omega}_*$ in (2.21) can be given as a mean over the spectrum

$$\tilde{\omega}_m = \frac{\int \tilde{\Omega}(\kappa)\tilde{\varepsilon}(\kappa) d\kappa}{\tilde{\varepsilon}} = a_\tau^{-2/19}\tau^{-q_\tau} B_{\beta_\tau}, \quad B_{\beta_\tau} = \frac{\int |\xi|\Phi_{\beta_\tau}(\xi) d\xi}{\int |\xi|^{1/2}\Phi_{\beta_\tau}(\xi) d\xi}, \tag{2.23}$$

or assuming

$$\max(\Phi_{\beta_\tau}) = \Phi_{\beta_\tau}(1) \tag{2.24}$$

as spectral peak frequency

$$\tilde{\omega}_p = a_\tau^{-2/19}\tau^{-q_\tau}. \tag{2.25}$$

From (2.14) for total input we have

$$\tilde{\Pi}(\tau) = a_\tau^{9/19}\tau^{s_p} C_{\beta_\tau}, \quad C_{\beta_\tau} = \int_{-\pi/2}^{\pi/2} \left(\beta_\tau |\xi|^{5/2} \frac{\partial\Phi_{\beta_\tau}}{\partial|\xi|} + \alpha_\tau |\xi|^{3/2} \Phi_{\beta_\tau} \right) d|\xi| d\theta. \tag{2.26}$$

The self-similarity parameter α_{ss} takes the following form (see (2.19))

$$\alpha_{ss}^{(d)} = \frac{A_{\beta_\tau} B_{\beta_\tau}^3}{C_{\beta_\tau}^{1/3}}. \tag{2.27}$$

Accepting spectral peak frequency ω_p as a characteristic one and using (2.20), we have a simpler expression

$$\alpha_{ss}^{(d)} = \frac{A_{\beta_\tau}^{2/3}}{p_\tau^{1/3}}. \tag{2.28}$$

In the case of (2.28), the self-similarity parameter $\alpha_{ss}^{(d)}$ depends explicitly on energy growth rate p_τ and on A_{β_τ} . An important feature of wave spectra – their

quasi-universality allows us to make analysis of the wave growth law (2.21) more transparent: it turns out that A_{β_τ} depends weakly on self-similarity index p_τ . We consider this point in presentation of numerical results.

2.2. Fetch-limited self-similar solutions

The case of fetch-limited growth (stationary, non-homogeneous Hasselmann's equation) can be analysed in a similar way (see for details Badulin *et al.* 2005b; Zakharov 2005b).

Consider an idealized problem of fetch-limited growth when constant offshore wind is perpendicular to the straight coast line and wind wave spectra depend on the only spatial coordinate x . Introducing non-dimensional fetch (see (2.3))

$$\chi = k_0 x.$$

look for self-similar solutions in the following form (cf. (2.5))

$$\tilde{n}(\mathbf{k}, \mathbf{x}) = a_\chi \chi^{\alpha_\chi} \Phi_{\beta_\chi}(\zeta, \theta), \quad \zeta = a_\chi^{1/5} \kappa \chi^{\beta_\chi}, \quad \zeta = |\zeta|, \quad \theta = \arctan(\zeta_x/\zeta_y). \quad (2.29)$$

The 'shape' function Φ_{β_χ} is determined by the integro-differential equation

$$\begin{aligned} & \frac{\cos \theta}{2\sqrt{\zeta}} \left[\alpha_\chi \Phi_{\beta_\chi} + \beta_\chi \zeta \frac{\partial \Phi_{\beta_\chi}}{\partial \zeta} \right] \\ &= 16\pi^2 \int |\tilde{T}_{\zeta_1 \zeta_2 \zeta_3, \theta_1 \theta_2 \theta_3}|^2 \zeta_1 \zeta_2 \zeta_3 d\zeta_1 d\zeta_2 d\zeta_3 d\theta_1 d\theta_2 d\theta_3 \delta(\zeta \cos \theta + \zeta_1 \cos \theta_1 \\ & \quad - \zeta_2 \cos \theta_2 - \zeta_3 \cos \theta_3) \delta(\zeta \sin \theta + \zeta_1 \sin \theta_1 - \zeta_2 \sin \theta_2 - \zeta_3 \sin \theta_3) \\ & \quad \times \delta(\sqrt{\zeta} + \sqrt{\zeta_1} - \sqrt{\zeta_2} - \sqrt{\zeta_3}) [\Phi_{\beta_\chi}(\zeta_1, \theta_1) \Phi_{\beta_\chi}(\zeta_2, \theta_2) \Phi_{\beta_\chi}(\zeta_3, \theta_3) \\ & \quad + \Phi_{\beta_\chi}(\zeta, \theta) \Phi_{\beta_\chi}(\zeta_2, \theta_2) \Phi_{\beta_\chi}(\zeta_3, \theta_3) - \Phi_{\beta_\chi}(\zeta, \theta) \Phi_{\beta_\chi}(\zeta_1, \theta_1) \Phi_{\beta_\chi}(\zeta_2, \theta_2) \\ & \quad - \Phi_{\beta_\chi}(\zeta, \theta) \Phi_{\beta_\chi}(\zeta_1, \theta_1) \Phi_{\beta_\chi}(\zeta_3, \theta_3)]. \end{aligned} \quad (2.30)$$

The condition of balance of total wave action

$$\langle \nabla_{\mathbf{k}} \omega_{\mathbf{k}} \nabla_{\mathbf{r}} N_{\mathbf{k}} \rangle = \langle S_{in} + S_{diss} \rangle \quad (2.31)$$

is consistent with solution (2.29) when the total wave action is a power function of fetch

$$\int \tilde{n}(\kappa, \chi) d\mathbf{k} = a_\chi^{3/5} \chi^{r_\chi} \int \Phi_{\beta_\chi}(\zeta) d\zeta. \quad (2.32)$$

Total energy obeys conditions of

$$\tilde{\varepsilon} = \int \tilde{\Omega}(\mathbf{k}) \tilde{n}(\kappa, \chi) d\mathbf{k} = a_\chi^{1/2} A_{\beta_\chi} \chi^{p_\chi}, \quad A_{\beta_\chi} = \int |\zeta|^{1/2} \Phi_{\beta_\chi}(\zeta) d\zeta, \quad (2.33)$$

and for mean frequency we obtain

$$\tilde{\omega}_m = \frac{\int \tilde{\Omega}(\mathbf{k}) \tilde{\varepsilon}(\mathbf{k}) d\mathbf{k}}{\tilde{\varepsilon}} = a_\chi^{-1/10} B_{\beta_\chi} \chi^{-q_\chi}, \quad B_{\beta_\chi} = \frac{\int |\zeta| \Phi_{\beta_\chi}(\zeta) d\zeta}{\int |\zeta|^{1/2} \Phi_{\beta_\chi}(\zeta) d\zeta}. \quad (2.34)$$

Accepting

$$\max(\Phi_{\beta_\chi}) = \Phi_{\beta_\chi}(1), \quad (2.35)$$

we have for peak frequency

$$\tilde{\omega}_p = a_\chi^{-1/10} \chi^{-q_\chi}. \quad (2.36)$$

The set of exponents obeys slightly different (if compared to the duration-limited case) relations between exponents α_χ and β_χ

$$\alpha_\chi = 5\beta_\chi - 1/2, \quad r_\chi = (3\alpha_\chi - 1)/5. \quad (2.37)$$

Linear relationship between wave growth p_χ and downshift exponents q_χ differs slightly from (2.10) for the duration-limited case

$$p_\chi = \frac{10q_\chi - 1}{2}. \quad (2.38)$$

For total energy and momentum exponents, we have (cf. (2.9a,b))

$$E_{tot} \sim \chi^{p_\chi}, \quad p_\chi = \alpha_\chi - 5\beta_\chi/2 = (10r_\chi - 1)/12, \quad (2.39a)$$

$$M_{tot} \sim \chi^{m_\chi}, \quad m_\chi = \alpha_\chi - 3\beta_\chi = (4r_\chi - 1)/6. \quad (2.39b)$$

The restriction on the exponents to provide a dominance of nonlinear transfer if compared with wave input and dissipation at infinitely long fetches gives (cf. (2.12))

$$\alpha_\chi > 1, \quad r_\tau > 2/5, \quad p_\tau > 1/4, \quad q_\tau > 3/20, \quad m_\tau > 1/10. \quad (2.40)$$

Even though the relationships for exponents of wave growth in duration-limited and fetch-limited cases (2.8), (2.7), (2.37), (2.38) are different, these exponents express the basic feature of the self-similar development: rigid link between wave spectra and spectral fluxes. The corresponding formulae can be easily derived as in previous sections. In terms of total energy and total flux at infinitely high frequencies, we have

$$\tilde{\varepsilon} \tilde{\omega}_*^4 = \alpha_{ss}^{(ff)} (\tilde{\omega}_*^3 \tilde{\Pi}(\chi))^{1/3}. \quad (2.41)$$

Having no arguments similar to those presented in figure 1 for duration-limited development, we cannot vouch for the equivalence of the self-similarity parameter $\alpha_{ss}^{(ff)}$ in (2.41) and $\alpha_{ss}^{(d)}$ in (2.19), (2.21). Moreover, turning to an ‘observable’ quantity – total wave input, we have to relate the total flux $\Pi(\chi)$ to convective derivative $\langle \nabla_k \omega_k \nabla_r N_k \rangle$ in (2.1), and hence to spatial derivative of total energy $\partial \varepsilon / \partial x$ and a characteristic group velocity. Finally, accepting the energy-input relation in a form similar to the duration-limited case, we obtain

$$\tilde{\varepsilon} \tilde{\omega}_*^4 = \alpha_{ss}^{(f)} \left(\frac{\tilde{\omega}_*^2}{2} \frac{\partial \tilde{\varepsilon}}{\partial \chi} \right)^{1/3} \quad (2.42)$$

or in dimensional form

$$\frac{\varepsilon \omega_*^4}{g^2} = \alpha_{ss}^{(f)} \left(\frac{\omega_*^2}{2g} \frac{\partial \varepsilon}{\partial x} \right)^{1/3}. \quad (2.43)$$

For peak frequency scaling (2.35), we have a simple formula for $\alpha_{ss}^{(f)}$ (cf. (2.28))

$$\alpha_{ss}^{(f)} = \frac{A_{\beta_\chi}^{2/3}}{p_\chi^{1/3}}. \quad (2.44)$$

Formally, within our analysis of self-similar solutions, we have

$$\alpha^{(d)} \neq \alpha^{(ff)} \neq \alpha^{(f)}.$$

Parameters $\alpha_{ss}^{(d)}$ and $\alpha_{ss}^{(ff)}$ are likely to be identical if we extend the particular spectrum-flux relations (2.19), (2.41) to the general case

$$\tilde{\varepsilon}\tilde{\omega}_*^4 = \alpha_{ss}(\tilde{\omega}_*^3\tilde{\Pi}(\tau, \chi))^{1/3} = \alpha_{ss}\left(\tilde{\omega}_*^3\frac{d\tilde{\varepsilon}(\tau, \chi)}{d\tau}\right)^{1/3}. \quad (2.45)$$

At the same time, we should be careful when relating $\alpha_{ss}^{(ff)}$ and $\alpha_{ss}^{(f)}$ because of the scaling of the convective derivative in (2.31) by the characteristic group velocity. Using self-similar scaling arguments only, we have

$$\langle \nabla_k \omega_k \nabla_r E_k \rangle \sim \frac{\omega_* \varepsilon}{2g}. \quad (2.46)$$

A similar trick is widely used in experimental studies when trying to treat one-point measurements as fetch-limited ones by means of time-to-space conversion and introducing a characteristic transport velocity (e.g. Hwang & Wang 2004). Here, we are aware of possible issues when using the group velocity to convert a duration-limited set-up to fetch-limited. Further, unless otherwise stated, we use notation α_{ss} irrespective the wave development set-up.

2.3. Self-similar solutions and experimental parameterizations of wind-wave spectra

Consistent use of the self-similarity analysis implies a presentation of results in terms of a minimal (and, at the same time, sufficient) number of non-dimensional physically relevant variables. In our case, it means the possibility of presenting solutions ((2.5), (2.29)) as time- (fetch-) independent. After trivial algebra, we come to a universal (valid for time- and fetch-duration set-ups) form of these solutions

$$\frac{\varepsilon(\omega, \theta)\omega_*^5}{g^2} = \alpha_{ss}\left(\frac{\omega_*^3 d\varepsilon/dt}{g^2}\right)^{1/3} \Phi_\beta(\omega/\omega_*, \theta). \quad (2.47)$$

Here, proper normalization is imposed for the shape function $\Phi_\beta(\omega/\omega_*, \theta)$ in order to satisfy wave growth relations ((2.20), (2.42)). Full derivative $d\varepsilon/dt$ and omission of scripts τ, χ are used to emphasize universality of this relation.

The found time-free (fetch-free) form of asymptotic self-similar solutions contains all the physical scalings of the split balance model ((1.2), (2.1)), i.e. can be considered as both physically and mathematically correct. Solution (1.9) is a direct analogue of weakly turbulent relations between spectral magnitudes and spectral fluxes represented by the Kolmogorov–Zakharov solutions (Zakharov & Filonenko 1966; Zakharov & Zaslavsky 1982), and parameter α_{ss} is a counterpart of Kolmogorov’s constants (Badulin *et al.* (2005a))

The self-similarity parameter α_{ss} and shape function Φ_β depend on growth rates ($p_{\tau(\chi)}$ or $q_{\tau(\chi)}$) as we see in (2.28), (2.43), but this dependence is quite weak. The latter feature – quasi-universality of spectral shapes is illustrated by the results of numerical solutions (figures 2 and 3) of the Hasselmann equation (1.3) in the duration-limited case for different wave inputs (Stewart 1974; Snyder *et al.* 1981; Plant 1982; Hsiao & Shemdin 1983; Donelan & Pierson 1987). Corresponding growth exponents p_τ vary in the wide range of $0.67 < p_\tau < 0.84$ (cf. (1.7)). Moreover, the scaling parameter a_τ responsible for spectra magnitudes (2.5) varies by 6 orders. Nevertheless, solutions keep to self-similar scaling (2.7) quite well.

Solutions (2.47) represent a typical second type (incomplete) self-similarity, when shape function Φ_β expresses a non-trivial dependence on an ‘internal’ variable – non-dimensional frequency, while ‘outer’ dependence is a ‘simple’ power-law function of non-dimensional wave input.

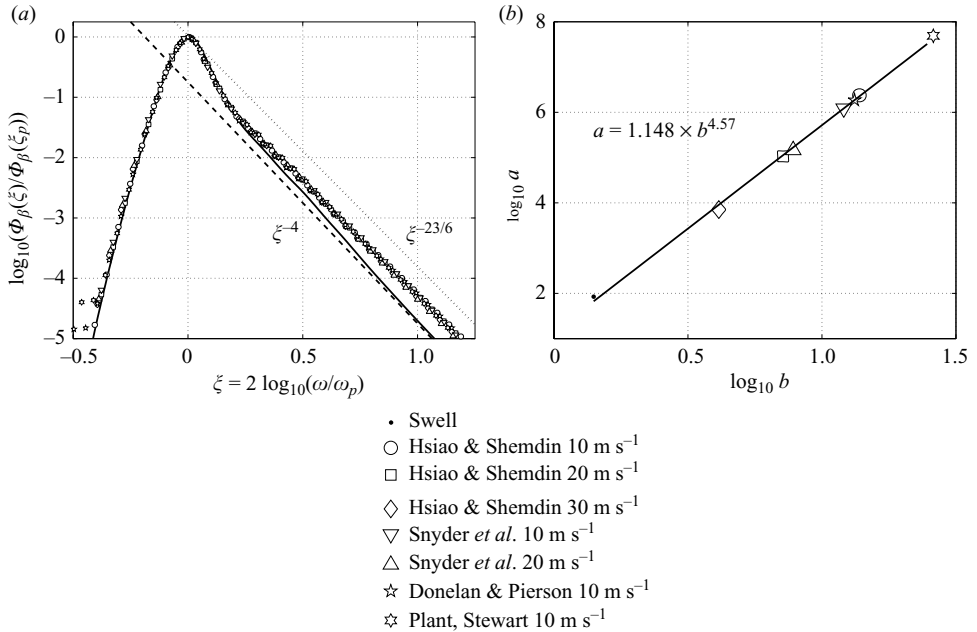


FIGURE 2. (a) Normalized spectral shape $\Phi_{\beta_r}(\xi)/\Phi_{\beta_r}(\xi_p)$ as a function of non-dimensional wave frequency for different wave inputs. The swell case is given by the solid line. (b) The scaling of the solution peaks and the peak positions. Fitting formula and the corresponding line are shown.

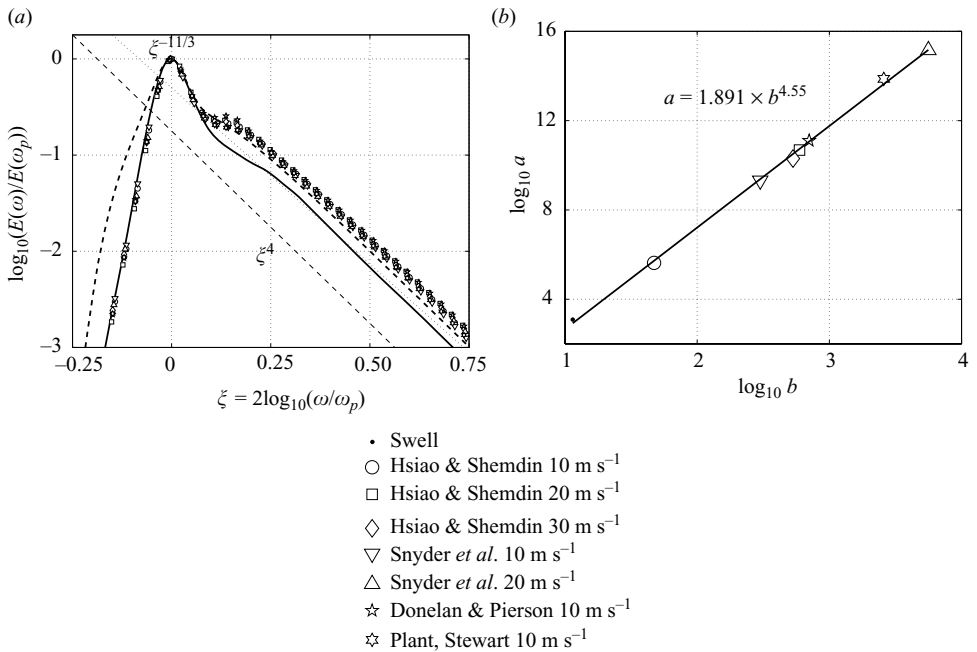


FIGURE 3. (a) Non-dimensional frequency spectrum $E(\omega)/E(\omega_p)$ as a function of non-dimensional wave frequency for different wave inputs. The JONSWAP spectrum shape for the standard enhancement $\gamma = 3.3$ is shown by the dashed curve, the swell shape is given by the solid line. (b) The dependence of the scaling parameters a_ω and b_ω , swell scaling is given by the dot.

It should be stressed that experimental parameterizations of wave spectra follow the same idea of incomplete self-similarity. A detailed discussion of this issue can be found in the JONSWAP report (Hasselmann *et al.* 1973): the original idea of similarity proposed by Kitaigorodskii (1962, 1983) was gradually converted into the idea of self-similarity of wind-wave spectra (see also Toba 1973*a, b*). In accordance with this idea, all the conventional parameterizations of wind-wave spectra postulate the self-similarity in the form of *incomplete or second-type self-similarity*

$$\frac{\varepsilon(\omega, \theta)\omega_p^5}{g^2} = \alpha_{exp}(C_p/U_h)^{\kappa_\alpha} \Phi_{exp}(\omega/\omega_p, \theta, \gamma, \sigma_a, \sigma_b, \dots), \quad (2.48)$$

with the corresponding duration- (fetch-) independent relationship for total energy

$$\frac{\varepsilon\omega_p^4}{g^2} = \alpha_{exp}(\gamma, \sigma_a, \sigma_b, \dots)(C_p/U_h)^{\kappa_\alpha}. \quad (2.49)$$

Additional parameters of the spectral shape Φ (in the JONSWAP model: spectrum enhancement γ , peak width parameters $\sigma_{a(b)}$) are widely used by experimentalists (e.g. Babanin & Soloviev 1998*a*) as tuning parameters. A unique choice of these parameters in (2.48) requires additional criteria when working with experimental data (excluding the basic one α_{exp} which is determined by total energy).

The most striking difference between theoretical parameterization (2.47) and its experimental counterpart (2.48) is in their outer scaling: the first one is scaled by non-dimensional wave input in full agreement with the split balance model (1.2), (2.1), while experimental form (2.48) uses traditional wave age scaling (1.6) introduced by Kitaigorodskii (1962).

The description of wave growth within the split balance model is complete as far as the total wave input is known. Adequate use of experimental wind speed scaling in (2.48) implies use of a model of wind-sea interaction necessary to convert characteristics of atmosphere into wave input quantities. In the absence of such a model, the self-similar parameterization can be considered as a simple fitting formula, but not as a physically relevant expression. This note is important in view of further attempts to propose a universal parameterization of wave growth dependencies in terms of wind speed (e.g. Wen *et al.* 1989, 1993; Goda 2003; Donelan *et al.* 1993). Using the words of Donelan *et al.* (1992) cited above we may say again:

‘Perhaps it is time to abandon the idea that a universal law of wave growth *in terms of wind speed scaling* is anything more than an idealization.’

The rigid weakly turbulent link of wave energy and total wave input (2.45) gives us a new understanding of the universality – the universal wave growth law (1.9). Building a bridge between experimental and theoretical approaches to the problem of wind-wave growth, we should realize, however, a conceptual difference of the two approaches.

Traditionally, the experimental search for wind-wave growth dependencies (1.4), (1.5) was undertaken for ‘correct’ values of exponents p_χ and q_χ (p_τ and q_τ) and corresponding pre-exponents of wave growth. Variations of $p_{\tau(\chi)}$ and $q_{\tau(\chi)}$ between the experiments were interpreted as an annoying feature which is due to either imperfect experiments (measurement limitations, natural data scatter, limited range of data and wind-wave conditions etc.) or deviations of the wave circumstances from so-called ‘ideal conditions’ of wave generation, development and propagation (see e.g. Kahma 1981). Many factors could contribute to the conditions of sea experiments not being a perfect fit to the idealized cases of duration- and fetch-limited growth.

For example, gustiness of the wind which is its inherent feature can lead to some 30–40% increase of the wave height (Abdalla & Cavaleri 2002). Non-stationarity of the wind speed (increasing or decreasing wind), temperature stratification, presence of swell, modulation of the wind stress by passing wave groups, or due to longer waves, or because of fine-scale inhomogeneity of wave skewness and asymmetry can all affect the wave growth rate, sometimes by a factor of 2–3 (e.g. Donelan *et al.* 2006). Many, if not most of these effects are usually present during field observations, but are routinely disregarded in experimental dependencies (1.4) and (1.5). All these and other effects are the ‘details’ of wind-wave interaction that should be incorporated into a corresponding physical model.

The proposed theoretical ‘flux scaling’ should be able to account (maybe somewhat indirectly) for all the ‘imperfect’ details of wind-wave growth. Deviations from the theoretical law (1.9), (2.47) can still be expected, for two reasons. (i) The asymptotic nature of the law: early stages of wave development do not obey the law. (ii) We have no reason to disregard a composite nature of the wave field owing to the broad range of wave scales: some parts of wave spectra can approach an asymptotic state and others cannot. The latter, in particular, can make our results somewhat sensitive to the choice, say, of characteristic frequency ω_* . Evidently, the frequency scaling should reflect the evolution of a ‘weakly turbulent core’ of wave field rather than the mean over all the scales: in the sense that peak frequency scaling looks more attractive if compared with a mean frequency one.

3. Duration-limited growth in numerical simulations

To check the validity of the weakly turbulent laws (1.9), we start with the duration-limited case. This case is extremely ‘inconvenient’ for field studies and the list of representative experiments is short. This will be compensated by results of an extensive numerical study (Badulin *et al.* 2005*b*). Experimental results on duration-limited growth will be discussed in a separate paper. Time series of the numerical experiments allow us to validate the weakly turbulent dependencies, first of all, in terms of relationships for self-similar solutions (2.10), (1.9) by simple fitting of the series with power-law dependencies as for (1.4). This somewhat restrictive approach can be avoided as far as we appreciate the fact of a weakly turbulent relationship between energy and flux (1.9) which does not imply any power-law dependence, but a tendency of wave spectra to an asymptotic behaviour controlled mostly by nonlinear transfer. We present this way of analysis as the *energy-flux diagram method*.

The key property of the split balance model – *independence of the wave growth on details of wave input function* – (Pushkarev *et al.* 2003; Badulin *et al.* 2005*b*) allows us to reproduce the self-similar power-law wave growth in the best way by using artificial source function S_f . Solutions with conventional input functions (Stewart 1974; Snyder *et al.* 1981; Plant 1982; Hsiao & Shemdin 1983; Donelan & Pierson 1987) allow us to quantify the departure from particular self-similar regimes and to make conclusions on the validity of weakly turbulent wave growth laws in the general case. The validity check for self-similar solutions consists of two parts. First of all, we check the link of exponents of total energy growth p_τ and of characteristic frequency downshift q_τ (2.10) following recent analysis of the fetch-limited growth (Zakharov 2005*b*). Secondly, we estimate the self-similarity parameter α_{ss} for different sets of p_τ , q_τ .

3.1. Exponents of duration-limited growth. Wave frequency scaling

The split balance model gives a family of solutions that depend on the self-similarity index p_τ . Exponents of total energy growth p_τ in numerical (Badulin *et al.* 2005*b*) and

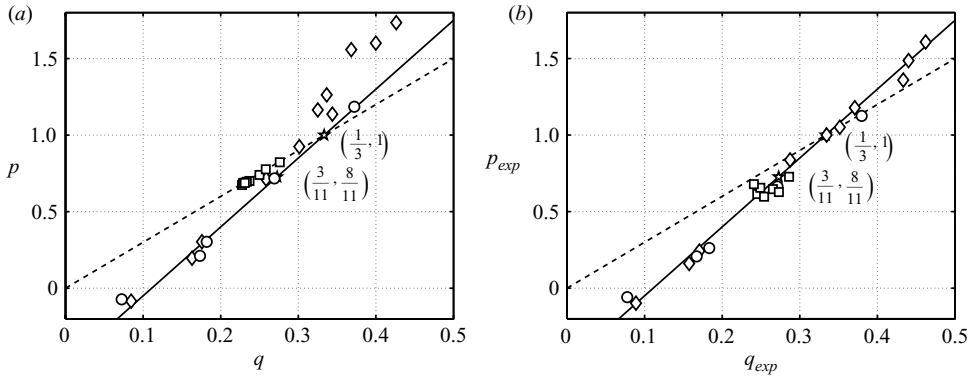


FIGURE 4. (a) Exponents p_τ and q_τ for power-law approximations of total energy and mean frequency of the kinetic equation solutions. (b) Exponents p_{exp} and q_{exp} derived from exponents of spectral peak growth α_τ and β_τ (see (2.7), (2.10)). \circ , runs with isotropic artificial increment (3.1); \diamond , runs with anisotropic artificial increment (3.1); \square , wave input given by conventional formulae (Stewart 1974; Snyder *et al.* 1981; Plant 1982; Hsiao & Shemdin 1983; Donelan & Pierson 1987). Sets of exponents for constant total wave action $(3/11, 8/11)$ and total wave energy $(1/3, 1)$ fluxes are given by stars. The solid line shows the theoretical dependence of p_τ on q_τ , the dashed line corresponds to Toba's $3/2$ law.

in sea experiments vary in a relatively narrow range (e.g. (1.7) for the fetch-limited case). Using the special set-up of numerical runs, we can try to cover an essentially broader range of the self-similarity index. It helps to detail important features of the problem discussed. In (Badulin *et al.* 2005b) such a set-up was presented as an 'academic' one.

The idea of this set-up naturally comes from the split balance model: since the wave development is determined primarily by total input (see (2.1)), we can put the wave input in a narrow high-frequency domain to free maximal space for inverse weakly turbulent cascading and the resulting self-similar solution. It is likely that self-similarity features will be better observable in this case.

The input is assumed to be linear in wave action (wave energy) with a time-dependent increment. Total energy grows as follows:

$$\frac{d\varepsilon}{dt} \sim \int_0^{2\pi} \int_{\omega_l}^{\omega_h} t^{p_{inc}-1} \varepsilon(\omega, \theta) d\omega d\theta, \quad (3.1)$$

where $(p_{inc} - 1)$ is the exponent of the wave energy increment. Note that exponent p_{inc} is not equal to the resulting exponent of total energy growth p_τ owing to the dependence of $\varepsilon(\omega, \theta)$ on time in the domain of wave input $\omega_l < \omega < \omega_h$.

In numerical runs with conventional formulae (Stewart 1974; Snyder *et al.* 1981; Plant 1982; Hsiao & Shemdin 1983; Donelan & Pierson 1987) wind input is distributed in a wide frequency domain and does not depend on time explicitly. In this case, total input depends on time owing to the interplay of spectral growth and downshift when the spectral peak moves to a range of lower wave increments. Generally, it leads to the total wave input decaying slightly with time. Accordingly, p_τ appears to be less than 1.

Figure 4 and table 1 show the dependence of the exponent of energy growth p_τ on q_τ . Numerical runs with artificial increments (3.1) give p_τ , q_τ varying in wide ranges

$$0.191 \leq p_\tau \leq 1.754, \quad 0.170 \leq q_\tau \leq 0.470, \quad (3.2)$$

Run	q_τ	p_τ	z_τ	ε_0	ω_0	$\alpha_{ss}^{(1)}$	$\alpha_{ss}^{(2)}$
ac 7/22	0.170	0.191	-0.049	1.534×10^{-1}	4.559	2.245	1.232
ac 5/11	0.181	0.303	-0.008	4.606×10^{-2}	5.203	1.283	1.086
ac 8/11	0.254	0.713	-0.047	4.106×10^{-4}	12.91	0.633	1.058
ac 19/22	0.289	0.924	-0.082	3.695×10^{-5}	19.72	0.416	1.038
ac 1	0.343	1.138	-0.063	3.282×10^{-6}	36.73	0.499	0.995
ac 47/44	0.355	1.169	0.048	8.647×10^{-8}	82.52	0.487	0.883
ac 25/22	0.366	1.256	0.073	1.164×10^{-8}	116.7	0.361	0.841
ac 17/11	0.470	1.754	0.093	1.649×10^{-10}	294.2	0.302	0.886
Snyder <i>et al.</i> 10 m s ⁻¹	0.247	0.669	0.038	6.740×10^{-4}	10.94	0.548	0.843
Snyder <i>et al.</i> 20 m s ⁻¹	0.300	0.835	-0.010	1.772×10^{-3}	10.84	0.944	0.858
Donelan 10 m s ⁻¹	0.243	0.694	0.067	5.848×10^{-4}	10.36	0.418	0.841
Hsiao & Shemdin 10 m s ⁻¹	0.247	0.685	-0.049	1.694×10^{-4}	14.50	0.504	0.878
Hsiao & Shemdin 20 m s ⁻¹	0.251	0.699	-0.046	2.303×10^{-3}	8.261	0.528	0.863
Hsiao & Shemdin 30 m s ⁻¹	0.263	0.734	-0.034	7.799×10^{-3}	6.635	0.607	0.855
Stewart 10 m s ⁻¹	0.281	0.759	-0.004	9.877×10^{-5}	19.58	0.838	0.794

TABLE 1. Exponents and pre-exponents (dimensional) of wind-wave growth and self-similarity parameter α_{ss} for numerical runs. The spectral peak frequency was used for scaling the self-similarity law (1.9). $q^{(1)}$ is the exponent of power-like approximation (1.4), $q^{(2)}$ is estimated from theoretical relation (2.10). Two different estimates of α_{ss} are given in accordance with formulae (3.4), (3.6). Series ‘ac’ are for artificial wave pumping exponents p_{inc} (3.1). Type of wave input parameterization and wind speed are shown for ‘realistic’ cases.

while for conventional wave input functions (Stewart 1974; Snyder *et al.* 1981; Plant 1982; Hsiao & Shemdin 1983; Donelan & Pierson 1987) this range is essentially narrower

$$0.669 \leq p_\tau \leq 0.835, \quad 0.243 \leq q_\tau \leq 0.300. \quad (3.3)$$

The case of swell (wave action $N_{tot} = \text{const}$) represents a special case of a self-similar solution.

First, p_τ , q_τ were estimated for total energy and mean-over-spectrum frequency ω_m (figure 4a). Generally, all the numerical points are slightly above the theoretical straight line (solid line in figure 4) both for conventional and artificial wave inputs. Moreover, for ‘realistic’ runs the points appear to be remarkably close to the Toba 3/2 law. The departure from the theoretical dependence can be explained easily if we take into account the asymptotic nature of the wave growth and the composite nature of the wave spectrum: different parts of the wave spectrum attain its self-similar regimes over different times or do not attain these regimes at all because of the different composition of wave input and nonlinear transfer. Thus, the resulting exponents p_τ , q_τ characterize both a self-similar ‘core’ and a non-self-similar ‘background’ (see §6.2.3 in Badulin *et al.* 2005b).

An alternative estimate of exponents p_τ , q_τ was targeted specifically to trace evolution of the self-similar ‘core’ of wave spectra. Exponent q_τ was estimated as $q_\tau = \beta_\tau/2$ (see (2.5)) by tracing the wave action peak frequency, and p_τ was found in a similar way from exponent α_τ of wave action magnitude growth (2.8). The new estimates of p_τ , q_τ collapse to the theoretical dependence fairly well (figure 4b).

Strong scatter of data points (figure 4a, especially for $p_\tau > 1$) for the case of artificial wave input, with respect to the theoretical line, shows a strong effect that the non-self-similar background of wave spectra has on exponents p_τ , q_τ . This cannot be avoided by special set-ups of numerical experiments. An adequate scaling of wave spectra

growth allows us to reveal self-similarity features of wave development: the spectral peak frequency, evidently, characterizes the self-similar core of wave spectra better than the mean frequency. This conclusion is valid for treatment of experimental results also: specific methods of measurement can emphasize spectral peak characteristics or, on the contrary, rely on the mean (integral) features. Thus, observations should be related very carefully to the theoretical predictions.

The numerical study allowed us to inspect a large domain of parameters where self-similar solutions are formally valid, i.e. $p_\tau > 4/19$, $q_\tau > 3/19$ (see (2.12) and § 5.2, equation 93 in Badulin *et al.* 2005*b*). The swell case was analysed as a specific case of ‘pure nonlinearity’. For conventional parameterizations of wind input and in the field experiments, exponent p_τ varies in a narrow range (compare (3.2), (3.3)). This in fact implies a significant scatter if a wave growth prediction is based on such dependencies for typical durations of a few hours. As mentioned above, for over 50 years the experimentalists have been struggling to reconcile the differences into a single purified universal dependence (see e.g. Wen *et al.* 1989; Kahma & Calkoen 1992). Now, based on our theory, it appears that the range of $0.6 \leq p_\tau \leq 1$ is not necessarily the experimental ‘scatter’, but is a natural subset of wave growth conditions allowed by the weakly turbulent self-similar development. More than that, the allowed range is much broader (i.e. $p_\tau > 4/19$ and an upper limit is determined by physically relevant magnitudes of wave growth only). Why has this broader range not been observed in the measurements? It is not because the slow growth of wave energy is ‘prohibited’ in nature. Very likely, it is either due to difficulties of observations of the corresponding stages of wave development or due to intentional filtering out the odd points by the experimentalists in their search for ‘ideal’ conditions of wave growth. Indeed, the extreme case of $p_\tau = 4/19$, for example, would correspond to the total wave energy input decaying as $\sim t^{-15/19}$ (see (2.10)). This would happen, for instance, if the wind was decreasing. Cases of the decreasing wind, however, were found to be significantly scattered with respect to the ‘ideal’ wave growth dependencies (Kahma & Calkoen 1992) and have been routinely discarded by the experimentalists as not suitable for such dependencies.

3.2. Method of energy-flux diagrams

The theoretical relationship for total energy and net wave input (2.21) being rewritten for power-law dependencies (1.4) gives a simple expression for α_{ss} in terms of dimensional pre-exponents ω_0 , ε_0

$$\alpha_{ss}^{(1)} = \left(\frac{\varepsilon_0^2 \omega_0^9}{p_\tau g^4} \right)^{1/3} t^{z_\tau} \quad (3.4)$$

where

$$z_\tau = \frac{2p_\tau - 9q_\tau + 1}{3}. \quad (3.5)$$

Superscript ‘(1)’ for α_{ss} is introduced for the particular case of power-law dependencies (1.4). Having independent estimates of exponents p_τ , q_τ , we generally have a dependence of $\alpha_{ss}^{(1)}$ on time. When exponents p_τ and q_τ satisfy the theoretical relationship (2.10), exponent z_τ vanishes and $\alpha_{ss}^{(1)}$ becomes time-independent. Thus, a consistent estimate of self-similarity parameter $\alpha_{ss}^{(1)}$ can be obtained by assuming one of the exponents of the wave growth ‘more reliable’ and using the theoretical relation to determine the other one. We shall refer to p_τ as a reference one unless otherwise stated. In fact, the departure of exponents from theoretical dependence is relatively

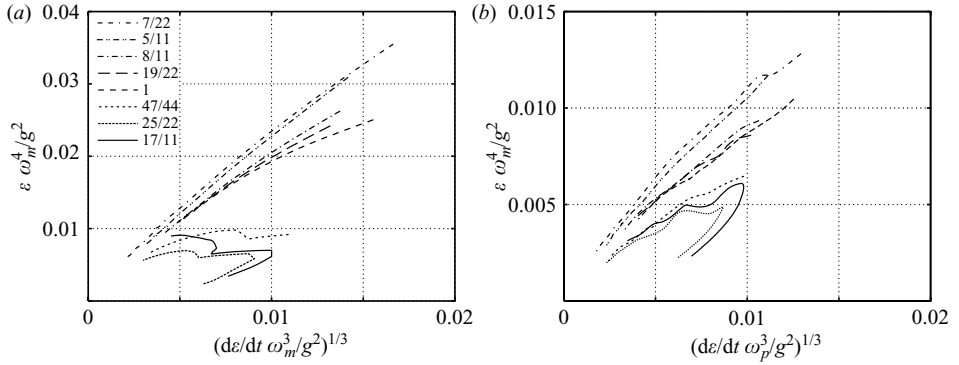


FIGURE 5. Energy-flux dependencies for different exponents of wave growth p_τ with artificial pumping (3.1) (p_{inc} are shown in the key). (a) Mean frequency is used for scaling, (b) peak frequency scales wave energy and wave energy flux. The tendency to the self-similarity law is seen much better in the latter case. Weak oscillations of trajectories at the bottom of the graphs are due to interpolation from the numerical grid. Trajectories are given for $t > 1800$ s.

small in our case: high power of ω_0 in (3.4) can affect the resulting estimates more strongly. A more general expression that does not imply power-law dependence of energy and characteristic frequency on time can be proposed in the following form (2.18),

$$\alpha_{ss}^{(2)} = \lim_{t \rightarrow \infty} \frac{\varepsilon \omega_*^3}{(g^4 d\varepsilon/dt)^{1/3}}. \quad (3.6)$$

Evidently, estimate (3.4), which contains an explicit dependence on time, implies additional error sources due to interpolation procedures, choice of initial time etc. Definition (3.6) looks more attractive and physically transparent as far as it is just a tangent of the plot of non-dimensional wave energy versus non-dimensional total wave input (1.9). Existence of the finite limit of $\alpha_{ss}^{(2)}$ can be considered as an independent argument for the validity of the split balance model and, hence, for the leading role of nonlinear transfer in wave spectra. It is useful to conduct a corresponding asymptotic analysis in terms of *energy-flux diagrams*

Figure 5 shows energy-flux dependencies for a series of numerical runs with artificial wave pumping (3.1). Wave input indexes p_{inc} (see (3.1)) are shown in the key. Mean frequency ω_m is used for scaling in figure 5(a) and the peak frequency ω_p in figure 5(b). The solutions evolve towards the coordinate origin with time. Trajectories show a clear tendency to linear dependence in both parts of figure 5 as is predicted by the weakly turbulent law (1.9). For mean frequency scaling (figure 5a), this tendency is slower and not so pronounced for $p_{inc} > 1$. Peak frequency scaling (figure 5b) supports the asymptotic law (1.9) more definitely. Note our ‘half-and-half solution’ of the scaling problem: we used peak frequency, but total, not peak (or ‘self-similar core’) magnitude of wave energy. It gives more regular dependencies for a rather poor numerical grid. In sea experiments, we have the same problem of observability and accuracy of different characteristics of wave field.

Figure 6 presents the energy-flux diagrams for different conventional parameterizations of wave input (Stewart 1974; Snyder *et al.* 1981; Plant 1982; Hsiao & Shemdin 1983; Donelan & Pierson 1987) for wind speeds $10 - 30 \text{ m s}^{-1}$. The same tendency to weakly turbulent energy-flux relationship (1.9) is seen remarkably well for both frequency scalings (mean frequency – figure 6a, peak frequency – figure 6b).

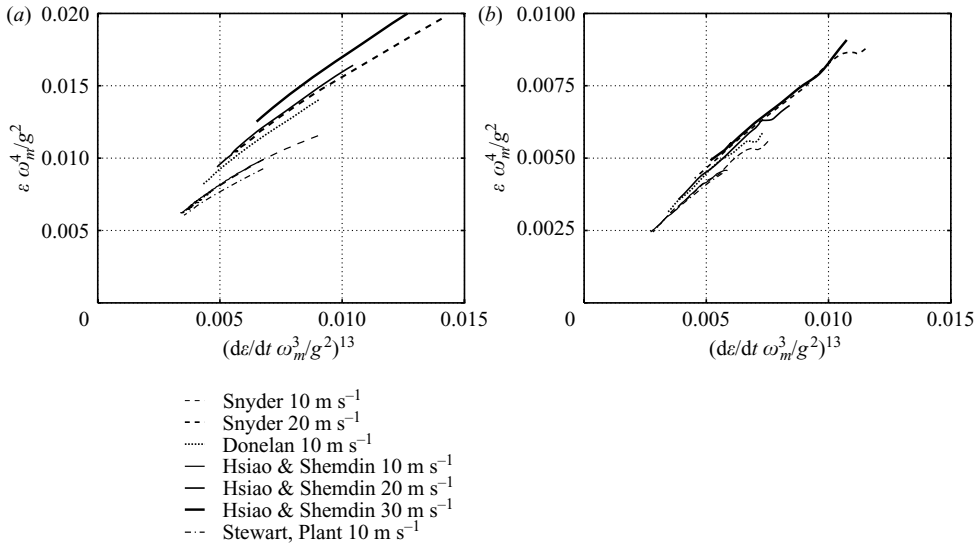


FIGURE 6. Energy-flux dependencies in ‘real’ numerical experiments for different parameterizations of wave input. (a) Mean frequency is used for scaling, (b) peak frequency scales wave energy and wave flux. Tendency to the self-similarity law is seen better for stronger winds and ‘more aggressive’ wave input functions (Snyder *et al.* 1981; Donelan & Pierson 1987). Trajectories are given for $t > 1800$ s.

As was expected, the asymptotic slope α_{ss} appeared to be very close for all the numerical experiments presented in figure 6 owing to the relatively low variability of exponent p_τ .

The attainability of the self-similar law (1.9) depends on total energy flux magnitude: for higher winds and stronger inputs (Snyder *et al.* 1981; Donelan & Pierson 1987) it is essentially faster than for winds of 10 m s⁻¹ and moderate wave increments (Stewart 1974; Hsiao & Shemdin 1983). We see again an illustration of the ‘magic circle’ effect: the weakly turbulent scenario works better when the wave input is stronger, the strong wave input provides a stronger self-similar core of wave spectra. The peak frequency scaling does not remove completely the effect of a non-self-similar background, but it reduces scatter of curves dramatically when compared with the mean frequency scaling.

As far as dissimilarity of artificial and ‘realistic’ runs is concerned, there is no essential difference in their tendency to the asymptotic behaviour. A special set-up of a numerical run can shorten, in some cases, time of relaxation to the asymptotic state due both to relatively small non-self-similar fraction of the resulting solution and to a generally higher (sometimes, intentionally too high) increment of wave growth.

3.3. Self-similarity parameter α_{ss} and pre-exponents of wind-wave growth

Table 1 summarizes results of the verification of the self-similarity law (1.9) for the duration-limited case. The downshift exponent q_τ was calculated from time evolution of the spectral peak, linear interpolation was used because of relatively poor frequency grid (71 points in the range 0.02 – 2 Hz) and slowness of downshift itself. Energy exponent p_τ is defined for total energy and, thus, cumulates evolution of self-similar core and non-self-similar background. Exponent z_τ (see (3.5)) represents deviation of p_τ , q_τ from the theoretical relationship (2.10). Pre-exponents ε_0 , ω_0 in (3.4) are given

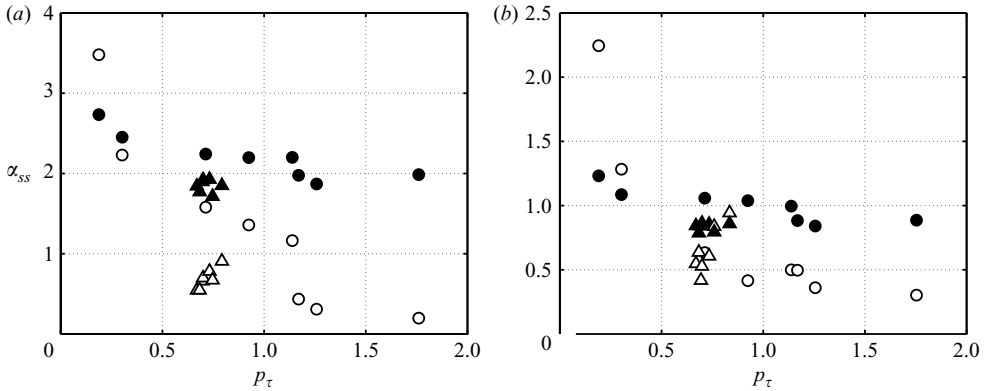


FIGURE 7. Self-similarity parameter α_{ss} for numerical solutions for duration-limited case. Circles, artificial pumping; triangles, conventional parameterizations of wave input at different wind speeds. (a) Mean frequency ω_m is used as a characteristic frequency in (1.9), (b) peak frequency ω_p scaling. Filled symbols correspond to estimates (3.6), open symbols to (3.4).

dimensional to avoid the problem of traditional wind speed scaling for artificial wave input (3.1).

Two last columns in table 1 give different estimates of self-similarity parameter α_{ss} by (3.4) and (3.6). These estimates are given in figure 7 for different frequency scalings ((a) mean frequency; (b) peak frequency). Peak frequency scaling and asymptotic estimate ((3.6), filled symbols in figure 7b) show more consistent results: we can see a gradual decay of α_{ss} with growing p_τ and essentially weaker dispersion if compared with estimate (3.4).

Estimate (3.4) is less reliable for two reasons. (i) The power-law fit is valid for large (formally infinite) times when approaching a self-similar regime. (ii) The initial time t_0 is not known for the asymptotic solutions: evidently, this time depends on the initial wave spectra, source function S_f etc.

Dependence $\alpha_{ss}(p_\tau)$ requires more comments in view of the above discussion on quasi-universality of wave spectra in §§ 2.1.2 and 2.3 (figures 2 and 3). Irrespective of the frequency scaling and definitions (3.4), (3.6) this dependence follows law $p_\tau^{-1/3}$ for $p_\tau > 0.5$ quite well (see figure 8). The latter means (see (2.28)) a weak dependence of A_{β_τ} , integral of energy spectral shape (2.22), on self-similarity index p_τ . Above, we presented this feature as quasi-universality of wave spectra. In figure 8, we show eyeball fits for both estimates of α_{ss} : $\alpha_{ss} = p_\tau^{-1/3}$ works well for the asymptotic formula (3.6), whereas fit $\alpha_{ss} = 0.45p_\tau^{-1/3}$ (3.6) approximates the estimate (3.4) derived from explicit time dependencies (1.4).

Slowly growing spectra (small p_τ) do not show this remarkable feature: their deviations from simple law $\alpha_{ss} \sim p_\tau^{-1/3}$ are quite large. It should be mentioned (see discussion of validity of approximate self-similar solutions in § 2.1 and (2.12)) that self-similarity features require high growth rates to ensure leading nonlinear transfer. For smaller rates, both self-similarity and quasi-universality features of the numerical solutions appear to be questionable.

4. Fetch-limited growth in field experiments

Experimental dependencies of wind-wave growth are the only background of our study of the fetch-limited case: up to now, no numerical results are available to verify

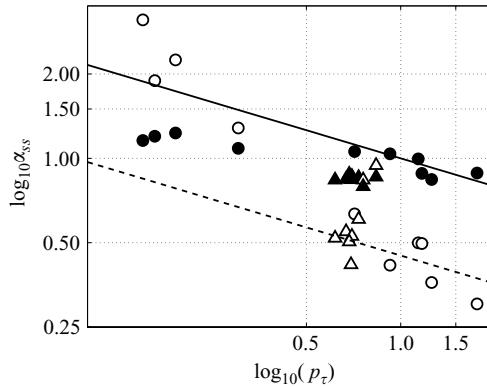


FIGURE 8. Self-similarity parameter α_{ss} for numerical solutions for duration-limited case. Circles, artificial wave pumping (3.1); triangles, conventional parameterizations of wave input at different wind speeds. Filled symbols correspond to estimates (3.6), open symbols to (3.4). Solid line, eye-ball fit $\alpha_{ss} = p_{\tau}^{-1/3}$ for (3.6); dashed line, $\alpha_{ss} = 0.45p_{\tau}^{-1/3}$ for (3.4).

self-similarity relationships (2.38), (4.1) in the same spirit as the above duration-limited case.

Over the years, a great number of field experiments have been undertaken to fit the evolution of total wave energy (wave variance) and peak or mean frequency with simple dependencies on non-dimensional fetch. Absolute majority of these integral dependencies correspond, as the authors claim, to an ideal stationary case of wave-field development in one spatial direction only, while conditions in the perpendicular direction remain homogeneous. Strictly speaking, only a part of these experiments can be explicitly regarded as the fetch-limited case: in some of them, the dependence on fetch was simulated by measuring the waves at a single point. Variation of the dimensionless fetch was often thus achieved by varying the wind speed rather than the wave fetch. Therefore, dependencies of the wave energy and the peak frequency on fetch are only as good as the correctness of the Kitaigorodskii (1962) scaling by the wind speed. The Kitaigorodskii scaling, in its turn, implies a universality of wind-wave interaction in terms of wind speed, i.e. independence of wave growth on additional physical properties such as stability of atmospheric boundary layer, presence of wave groups etc.

The idea of universality, broadly employed, corrupted and concealed the true experimental wave growth dependencies. First of all, results of measurements at different conditions are often combined to derive 'more statistically reliable' wave-growth dependencies. Secondly, data are treated as fetch-limited by enforced use of time-to-space transformation of time series measured in a single point. Finally, essential wind-wave physics is ignored when waves in laboratory tanks and at sea are competing on equal terms in combined data sets for describing the wave growth dependencies.

Thus, all the characteristics of the available experimental data require a thorough revision before we try to use them in order to verify the theoretical wave-growth law (1.9). Here, we analysed all dependencies available to us obtained over more than 50 years, and every set went through thorough and detailed scrutiny before being accepted or rejected for further comparisons.

Not all of the dependencies are expected to conform to the theory presented in this paper. As detailed below, the theory is, for example, not applicable to laboratory

conditions. Another big issue is the traditional scaling by the wind which is embedded in all integral dependencies available at present. The wind is an irrelevant parameter for the weak-turbulence approach, but we cannot un-scale the experimental data and remove the wind. Rather, we have to deal with the dependencies as they are. Therefore, we scrutinize every single experimental study and remove dependencies where the spurious correlations due to wind scaling, inclusion of the laboratory data or other factors may have essentially affected the growth exponents.

These and other characteristics were analysed, and records which correspond to self-similar wave development (from the point of view of the weak turbulence) were selected. Such records form approximately half of the total number of data sets available. Other records are also not simply thrown away, but will always be shown in the background.

Analysis by Zakharov (2005*b*) demonstrated that exponents of the fetch-limited growth dependencies follow the self-similarity relationship (2.38) remarkably well for six fetch-limited experiments. As mentioned above, it is not the case for the comprehensive set of experiments presented in this paper. Moreover, for two-thirds of the cases selected by Zakharov (2005*b*), a coincidence rather than a firm agreement takes place: methods of measurements and data analysis could have corrupted the ‘true’ wave-growth dependencies in those records significantly.

At first glance, the experimental data presented as power-law approximations (1.5) are ‘ready-to-use’ for verification of the theoretical results. First of all, the exponents p_χ , q_χ are provided in explicit form and the corresponding theoretical linkage of these exponents (2.38) can be checked trivially in the spirit of Zakharov (2005*b*). Secondly, the total wave input $d\varepsilon/dt$ (the convective derivative) can be calculated analytically. In non-dimensional variables with constant scales of energy, frequency and fetch, it gives (compare (3.4))

$$\alpha_{ss}^{(f)} = \left(\frac{2\varepsilon_0^2 \tilde{\omega}_0^{10}}{p_\chi} \right)^{1/3} \chi^{z_\chi}, \quad (4.1)$$

where

$$z_\chi = \frac{2p_\chi - 10q_\chi + 1}{3}. \quad (4.2)$$

Formula (4.1) for the self-similarity parameter α_{ss} in fetch-limited cases looks similar to the duration-limited one (3.4) and becomes fetch-independent when the theoretical relationship for exponents p_χ , q_χ is satisfied, i.e. z_χ in (4.2) vanishes. It should be stressed that, in order for (4.1) to be unambiguously obtained from the experimental dependencies, the latter are required to be scaled by a constant value of wind speed U_h . Instead, the crafty scaling of wave data by instantaneous wind speed or other parameters of air–sea interaction (Davidan 1996) in the available results of field observations hinders correct weakly turbulent wave physics and makes relationships (2.38), (4.1)) useless or hard to employ.

Therefore, returning to the problem of inadequate scaling of wind-wave data by wind speed, we see that dimensional raw data are more useful in our case, but, generally, unavailable. Thus, in our analysis, we are deprived of such a vivid tool as energy-flux diagrams used in the previous section. As an indemnity we have one positive feature of the fetch-limited set-up (we mean, obviously, ‘true’ set-up – fetch-limited measurements along a number of spatially distributed points): such a set-up has a reference point – a coastline where the wind blows from. It cannot resolve completely the problem of the correct account of the initial stage of wave

Experiment	$\tilde{\varepsilon}_0 \times 10^7$	p_x	$\tilde{\omega}_0$	q_x	z_x
1.1 Black Sea (Babanin & Soloviev 1998 <i>b</i>)	4.41	0.89	15.14	0.275	0.010
1.2 Walsh <i>et al.</i> (1989) US coast	1.86	1.0	14.45	0.29	0.033
1.3 Kahma & Calkoen (1992) unstable	5.4	0.94	14.2	0.28	0.027
1.4 Kahma & Calkoen (1992) stable	9.3	0.76	12.0	0.24	0.040
2.1 Dobson <i>et al.</i> (1989)	12.7	0.75	10.68	0.24	0.033
2.2 Kahma & Pettersson (1994)	5.3	0.93	12.66	0.28	0.020
2.3 JONSWAP by Davidan (1980)	4.363	1.0	16.02	0.28	0.067
2.4 JONSWAP by Phillips (1977)	2.6	1.0	11.18	0.25	0.167
2.5 Kahma & Calkoen (1992) composite	5.2	0.9	13.7	0.27	0.033
2.6 Donelan <i>et al.</i> (1985)	8.41	0.76	11.6	0.23	0.073
2.7 CERC (1977) by Young (1999)	7.82	0.84	10.82	0.25	0.060
3.1 Wen <i>et al.</i> (1989)	18.9	0.7	10.4	0.233	0.023
3.2 Evans & Kibblewhite (1990) neutral	2.6	0.872	18.72	0.3	-0.085
3.3 Evans & Kibblewhite (1990) stable	5.9	0.786	16.27	0.28	-0.076
3.4 Kahma (1981, 1986) rapid growth	3.6	1.0	20	0.33	-0.100
3.5 Kahma (1986) average growth	2.0	1.0	22	0.33	-0.100
3.6 Donelan <i>et al.</i> (1992) St Claire	1.7	1.0	22.62	0.33	-0.100
3.7 Hwang & Wang (2004); Hwang (2006)	6.19	0.81	11.86	0.237	0.084
3.8 Ross (1978), Atlantic, stable	1.2	1.1	11.94	0.27	0.167
3.9 Liu & Ross (1980), Michigan, unstable	0.68	1.1	12.88	0.27	0.167
3.10 Liu & Ross (1980), our fit (see figure 10)	77	0.52	2.36	0.08	0.413
3.11 Davidan (1996) for u^* scaling	794.0	1.0	9.160	0.34	-0.133
4.1 JONSWAP (Hasselmann <i>et al.</i> 1973)	1.6	1.0	21.99	0.33	-0.010
4.2 Mitsuyasu <i>et al.</i> (1971)	2.89	1.008	19.72	0.33	-0.095

TABLE 2. Exponents and pre-exponents of wind-wave growth in fetch-limited experiments. Cases studied in Zakharov (2005*b*) are given in bold.

development, but the problem itself appears to be not so critical as in the duration-limited case: at the initial stage, waves are relatively short and, hence, slow. Thus, the initial stage for the fetch-limited case is relatively short if compared to the duration-limited case. We cannot appreciate the value of this fact in its full extent: numerical study of fetch-limited development has not been done so far and the experimental data are too coarse to identify different stages of wind-wave development.

4.1. Experimental dependencies of fetch-limited wind-wave growth

In this paper, we analyse all available dependencies of total wave energy and wave frequency collected in fetch-limited experiments over the past 50 years or so. As mentioned above, these dependencies should go through a thorough revision before they can be used for comparisons as not all of them are expected to conform with the theory. We analyse every available experimental dependence set, show its conformance with theoretical predictions and try to understand why, in some cases, there is no such conformance and, in other cases, there are deviations and scatter around the theoretical lines. All the dependencies are listed in four groups (see tables 2 and 3) and the corresponding results are presented in different panels in figures 9 and 11. We tried to follow formal criteria when creating these lists. Sometimes these criteria were difficult to relate to particular experimental cases. Thus, the proposed range of the experiments is, to some extent, arbitrary and breaks between groups are not so strict.

The first list (group 1 in tables 2 and 3) presents the ‘cleanest’ (from the point of view of our theory) results. Within the first group, we shall refer to the Black Sea experiment (Efimov, Krivinski & Soloviev 1986; Babanin & Soloviev 1998*b*) as a

Experiment	p_χ	z_τ	α_{ss}
1.1 Black Sea (Efimov <i>et al.</i> 1986)	0.89	0.010	0.652
1.2 Walsh <i>et al.</i> (1989), US coast	1.0	0.033	0.302
1.3 Kahma & Calkoen (1992) unstable	0.94	0.027	0.591
1.4 Kahma & Calkoen (1992) stable	0.76	0.040	0.520
2.1 Dobson <i>et al.</i> (1989)	0.75	0.033	0.436
2.2 Kahma & Pettersson (1994)	0.93	0.02	0.400
2.3 JONSWAP by Davidan (1980)	1.0	0.067	0.751
2.4 JONSWAP by Phillips (1977)	1.0	0.167	0.160
2.5 Kahma & Calkoen (1992) composite	0.90	0.033	0.519
2.6 Donelan <i>et al.</i> (1985)	0.76	0.073	0.435
2.7 CERC (1977) by Young (1999)	0.84	0.060	0.318
3.1 Wen <i>et al.</i> (1989)	0.7	0.023	0.533
3.2 Evans & Kibblewhite (1990), neutral	0.872	-0.085	0.936
3.3 Evans & Kibblewhite (1990), stable	0.786	-0.076	1.048
3.4 Kahma (1981, 1986) rapid growth	1.0	-0.100	1.385
3.5 Kahma (1981) average growth	1.0	-0.100	1.286
3.6 Donelan <i>et al.</i> (1992)	1.0	-0.100	1.266
3.7 Hwang & Wang (2004), Hwang (2006)	0.81	0.084	0.373
3.8 Ross (1978), Atlantic, stable	1.1	0.167	0.116
3.9 Liu & Ross (1980), Michigan, unstable	1.1	0.167	0.102
3.10 Liu & Ross (1980), our fit (see figure 10)	0.52	0.413	0.011
3.11 Davidan (1996) for u^* scaling	1.0	0.340	3.743
4.1 JONSWAP (Hasselmann <i>et al.</i> 1973)	1.0	-0.100	1.106
4.2 Mitsuyasu <i>et al.</i> (1971)	1.008	-0.095	1.138

TABLE 3. Exponent p_χ of wind-wave growth and self-similarity parameter α_{ss} in fetch-limited experiments for the observed p_χ and theoretical value of q_χ^{th} (2.38), z_τ is detuning exponent in formula for self-similarity parameter α_{ss} (4.1). Cases by Zakharov (2005*b*) are given in bold.

reference one, mainly, because the raw data are available for re-analysis. Also, the Black Sea growth dependencies agree most closely with the theoretical predictions. All other series of the group are based on measurements at a number of points: the dependence on non-dimensional fetch was not simulated by variation of the wind speed. Additionally, they correspond to relatively homogeneous conditions of wave growth and measurements.

The series of the second list were obtained in fetch-limited experiments in a number of points and, in this sense, they are similar to those of the first list. At the same time, they may suffer some lack of accuracy in terms of our theory, first of all, owing to composite data sets for different conditions of wave development following the idea of an ‘ideal’ set of wave growth exponents p_χ , q_χ and attempting to have ‘statistically more reliable results’. Results of this group can be used for our analysis with some caution. As will be seen, they demonstrate a reasonably good conformance with the theoretical predictions.

The third list is an antagonist of the first two groups: the collected dependencies were obtained for composite data sets and used one-point measurements with further conversion into dependencies on dimensionless fetch by varying the wind speed. These data are not expected to conform to our theory and therefore should not be used for comparison and verification of the dependencies for the self-similar wave growth. Also, parameterizations where the exponents were presumed on a basis of some grounds or considerations, and the dependencies were forced to fit these exponents,

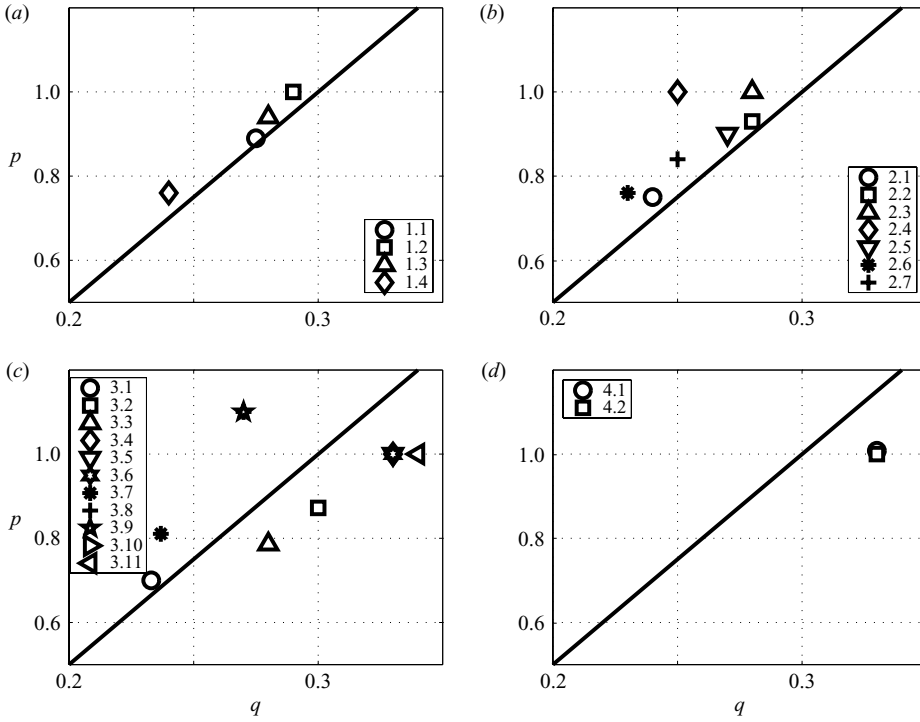


FIGURE 9. Dependence of p_χ on q_χ for different groups of fetch-limited experiments (§§ 4.2.1–4.2.4). Solid line, theoretical dependence $p_\chi(q_\chi)$ (2.38) for fetch-limited growth. Symbols for experiments collected in table 2 are given in keys.

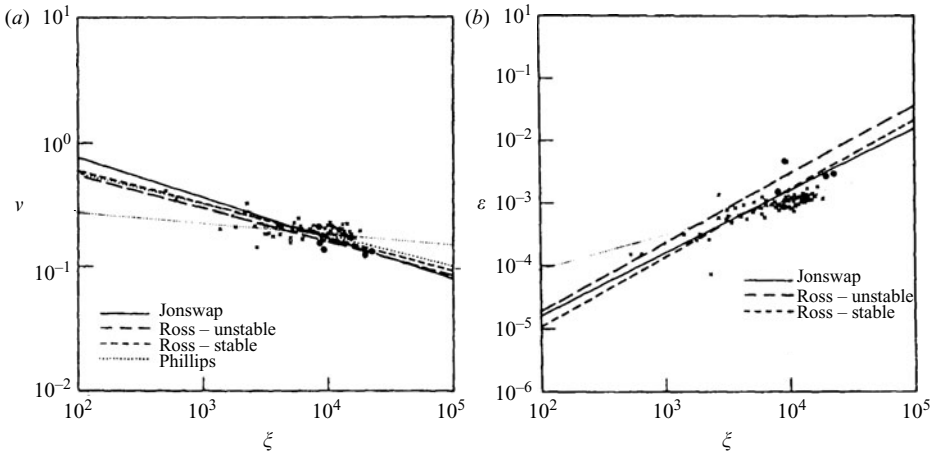


FIGURE 10. Figures 4 and 5 by Liu & Ross (1980). The line with essentially smaller tangent corresponds to our best fit.

were placed into this group. Obviously, such presumed exponents may correspond to the theoretically expected exponents only by coincidence.

The last group comprises of two, maybe the most respected experimental works on wave growth by Mitsuyasu, Nakamura & Komori (1971) and Hasselmann *et al.* (1973). The formal reason for their low ranking is the use of laboratory measurements. Tank

data are embedded in these experimental dependencies where they are combined with the field data. Laboratory waves, however, correspond to very short fetches (a few hundred wavelengths at best) and thus cannot be directly related to the open sea conditions as their physics is quite different. The kinetic description (the Hasselmann equation) is not applicable to such waves, both because of the short time of wave development and due to the quasi-unidirectional propagation where the essentially two-dimensional four-wave resonances responsible for nonlinear transfer can be suppressed or modified.

The dependencies from Zakharov (2005*b*) are given in bold in tables 2 and 3. Note, that only two of these six dependencies fall into the ‘good lists’.

4.2. Exponents of wind-wave growth in fetch-limited experiments

As in the analysis of the duration-limited case, we follow a series of validity checks to show conformance of experimental results to theoretical predictions. The results of the first check, exponents of wind-wave growth, are presented in table 2 and in figure 9. The exponents for the four groups are given in different panels in figures and the keys correspond to the numbering in tables 2 and 3.

4.2.1. Group 1. ‘The cleanest’ dependencies

The first group (1.1–1.4 in table 2) demonstrates the best conformance with the theoretical link of exponents p_χ , q_χ and a slight overestimate of exponent p_χ when compared with its theoretical values. This positive bias p_χ value is reproduced in the fetch-limited experiments of group 2 as well and in the duration-limited numerical runs (see figure 4) and can possibly be explained by the effect of the widening of developing wave spectra. Such widening would cause a relatively more rapid growth of the wave variance and, therefore, somewhat larger, with respect to the theory, exponent p_χ . This widening is confirmed by many observations (e.g. Babanin & Soloviev 1998*b*) and can be, for example, characterized by the spectral width parameter ν as follows (Belberov *et al.* 1983)

$$\nu = \frac{\varepsilon}{\omega_p \varepsilon(\omega_p)}.$$

Experimental studies give an integral estimate of ν only, but not details and physical mechanisms of the widening. Analysis of our numerical runs shows that the spectral ‘core’ keeps its shape quite well in the process and the widening is mainly due to the non-self-similar background. In groups 3 and 4, this fine effect is likely to be buried in the noise resulting from inclusion of composite, laboratory data sets (group 4) or from the one-point measurements with questionable time-to-fetch conversion of the time series (Evans & Kibblewhite 1990; Davidan 1996). Consequently, the data points of these groups are scattered around the theoretical curve rather than being above the line.

Note, that results of the Black Sea experiment, airborne measurements in the North Atlantic (Walsh *et al.* 1989) and the Bothnian Sea observations (Kahma & Calkoen 1992) produce very different p_χ and q_χ exponents while being quite close to the theoretical line. Thus, they demonstrate the universality of the wave-growth dependencies in the sense of the weakly turbulent law (1.9), but not in the rigid framework of the ‘experimental tradition’.

We speculate here, within the proposed theory, on the differences between wave development under different atmospheric stabilities. First of all, the observed difference justifies once more the inadequacy of wind speed scaling: at close magnitudes of the

wind speed, the exponents and pre-exponents of wave growth are essentially different (compare pairs of dependencies by Kahma & Calkoen 1992, in table 2), development under unstable stratification being faster. The explanation can be found in terms of flux dependence on wave development. The wave growth depends crucially on the wave-induced turbulent pulsations of pressure in the air, their magnitude and coherence with the wave slope. Under the unstable conditions, convective turbulence is additionally superposed over such wave-induced turbulence and reduces the coherence of the pressure pulsations with wave slope. This should lead to a reduction of the wind input compared to the stable conditions at early stages of wave development (small waves). As the waves grow, the magnitude of the wave-induced turbulence increases, whereas magnitude of the convective turbulence remains relatively constant. Therefore, for the unstable conditions, as the waves grow, the relative wind input grows faster (or decays slower) if compared to the stable conditions. According to the presented theory this should lead to greater values of exponent p_x (see above) which is indeed observed in the experiment. Thus, the theory not only allows us to predict the behaviour of the growth exponents and justify the variability of these exponents between different experiments, but also explains qualitative peculiarities of such growth, such as those differences between growth in stable and unstable conditions, between growth at constant, rising and decreasing winds.

4.2.2. Group 2. Composite data

Reasons for possible deterioration of group 2 are intimately connected with the key issue of our analysis: scaling of wind-wave growth. Such scaling applied by different authors to their original data in order to obtain non-dimensional dependencies typically involves wind speed as an external parameter, whereas within our approach the self-similar behaviour is controlled by intrinsic wave-field properties and has to be scaled by the corresponding external parameter – total net input (see (2.1)). The wind and the net wave input are not completely independent, and that is why the Kitaigorodskii-like scaling has been successful to an extent so far, with obvious limitations in many cases. However, the wind and the net wave input are not directly and unambiguously related either. Therefore, the wind scaling can corrupt our weakly nonlinear physics in two ways: first, by using instantaneous wind speed, as was criticized above, and secondly, by collecting data from different sources. The latter is often done in order to have a ‘more representative’ set in terms of the Kitaigorodskii approach, but such a compilation may prove unsuitable for the weak-turbulence theory. Data for different conditions of air–sea interaction (atmosphere stability, gustiness etc.) and hence for different rates of wave growth being put together are not supposed to satisfy our theoretical relationships.

The ‘representativeness’ of wave growth dependence by Dobson *et al.* (1989) (case 2.1 in tables 2 and 3) has been achieved by collecting data for different directions with respect to the shoreline. Authors themselves stress a pronounced difference of wave growth for the different directions (see figure 6 in Dobson *et al.* 1989). The feature that makes this work useful for our analysis is the fetch-averaged wind speed used for data scaling (point 1 in Concluding remarks of Dobson *et al.* 1989). Authors came to this decision because of the absence of reliable *in situ* wind data and considering that ‘the fetch-averaged wind must represent a time and space history of the wave field’. Note, that exponents of wave growth for this case conform the theoretical relationship (2.38) quite well. Nevertheless, we put this case into group 2 for formal reasons: composite data were used for deriving wave growth dependencies.

Kahma & Pettersson (1994) and Pettersson (2004) had the same problem for their data collected in a broad range of fetches and with various shoreline geometry in the Baltic Sea. Despite formally good conformance of power-law fits with previous results by Kahma & Calkoen (1992) (and with our theoretical relationship (2.38)), the authors found a strong scatter of experimental points. Their conclusion (Kahma & Pettersson 1994, p. 262) that ‘the effective fetch concept is a poor approximation’ agrees with our point: wind speed and fetch are not the only physical parameters that determine air–sea interaction and the resulting wave growth. This conclusion is best supported by the study for narrow bays (Kahma & Pettersson 1994) where conditions of air–sea interaction can vary dramatically.

The most representative collections (cases 2.3, 2.4) are based on subsets of JONSWAP data (Hasselmann *et al.* 1973). Kahma & Calkoen (1992) in their thorough investigation of differences between various parameterizations of wave integral properties demonstrated that, for JONSWAP data, many ‘noisy’ spectra were included. When we (not Kahma & Calkoen 1992) call these spectra ‘noisy’ we do not mean measurement noise. As Kahma & Calkoen (1992) describe it: ‘many of the spectra from the JONSWAP experiment show more structure’ compared to other experiments, i.e. their form is often not that due to generation by the wind only, but reveals the presence of mixed seas, swell etc. Also, cases of gusty, constant, rising and decreasing winds were not separated, neither were situations of stable and unstable stratification. In terms of our approach this means mixing together occurrences of different growth parameters, which leads to an unpredictable average. Once Kahma & Calkoen (1992) performed the separation of different subsets within JONSWAP data, scatter of the reanalysed data significantly decreased and parameters of the dependencies noticeably changed.

Case 2.5 shows an additional example of composite data sets. Stable and unstable data (cases 1.3 and 1.4) mixed together into a composite data set (case 2.5 in table 2) produce an intermediate result. The resulting exponents appear to be closer to the unstable case than to the stable case.

Scatter of Donelan *et al.* (1985) data (case 2.6) was discussed in detail by Kahma & Calkoen. They argued that this data set could have an additional scatter because the stable and unstable stratification data points were used together. Kahma & Calkoen (1992) also pointed out that the Lake Ontario p_χ could have suffered an additional loss of accuracy because Donelan *et al.* (1985) did not obtain it directly and therefore for their data it is derived from the energy versus peak frequency dependence, which is subject to strong spurious correlations.

The SMB data (case 2.7) were obtained in the early years of wave research, soon after the Second World War and are reported here as they are formulated by Young (1999). In those days, measurements and data-processing procedures were far less accurate than they are now and even were in the 1970s. The results were summarized in CERC (1977) where dependencies of dimensionless energy and peak frequency on dimensionless fetch were expressed in terms of functions of hyperbolic tangent. The power-law functions quoted here were then obtained as asymptotic forms of the tangent functions. After so many manipulations, the SMB CERC curves can be expected to produce some lack of accuracy. In fact, they behave surprisingly well, particularly if compared to those obtained in the 1970s and early 1980s. One possible reason for such a good conformation with the sophisticated measurements of late 1980s and 1990s is that, because of very limiting data recording and processing capacities, bulk processing was not possible and therefore the data would go through careful selection.

4.2.3. Group 3. 'Bad' dependencies

Dependence by Wen *et al.* (1989) is the closest outlier in terms of the theoretical exponents p_χ , q_χ . It was obtained as a mean dependence over five empirical dependencies including cases 4.1 (Hasselmann *et al.* 1973) and 2.3 (Davidan 1980) considered here and formulae adopted by the national coastal engineering committees of USSR, USA and China. The idea of 'universal' wave-growth law has been realized in this paper in its extreme form by collecting and averaging a number of possible dependencies. We should mention that averaging parameters of parameterizations based on different data sets, rather than combining the data sets in order to obtain an average parameterization, is a questionable approach for statistics, but as we said in this paper, we are attempting to analyse all published wave-growth dependencies.

Two points from the Evans & Kibblewhite (1990) experiment (cases 3.2 and 3.3) lie below the theoretical line and therefore, if our approach is right, it is most likely that the dependence of peak frequency on fetch is too strong (i.e. exponent q_χ is too large). The two points correspond to different stratifications and the data as such went through very thorough selection and only 'clean' spectra of purely wind-generated waves with known fetch were selected. This dimensional fetch, in fact, was almost always the same, some 200 km, and since the measurements were made from a stationary platform, this is a classical case when variation of the dimensionless parameters was achieved mostly because of variation of the wind. In such cases, as Kahma & Calkoen (1992) pointed out, since all the dimensionless parameters depend on the wind speed, spurious correlations may arise: 'if the common variable is inaccurate and all the other variables are nearly constant, the correlation between the dimensionless variables can be entirely spurious'. According to Kahma & Calkoen (1992), for peak frequency on fetch dependence, such a spurious correlation would lead to $q_\chi = 1/2$. If the correlation is only partially spurious, it would, apparently, tend to overestimate the values of q_χ which naturally are expected in the range $q_\chi = 1/4$ to $q_\chi = 1/3$. This is most probably what happened, particularly as the wind over 200 km fetch could hardly have been measured with great precision. It is important to mention that, according to Kahma & Calkoen (1992), the variance-on-fetch dependence is much less subject to the spurious correlations.

Another set of $p_\chi = 1$ and $q_\chi = 1/3$ dependencies, those by Kahma (1981, 1986) (cases 3.4 and 3.5) appear to have had their exponents forced to the fixed values in an attempt to evaluate the respective pre-exponents. The enforcing was justified on the basis of semi-empirical considerations of assumed growth behaviour of assumed spectral shapes. Kahma & Calkoen (1992) later revisited the same data set and, based on the statistical fit, produced power-law dependencies discussed in list 1 of table 2 (cases 1.3 and 1.4).

Dependence 3.6 by Donelan *et al.* (1992) similarly to the above case (Evans & Kibblewhite 1990) is based on one-point measurements and suffers the same problem of spurious correlations of the resulting non-dimensional energy, frequency and fetch. Additionally, the choice of energy-growth exponent has been partially enforced by the JONSWAP results following the idea of the universality of wave growth. The paper is concluded by a remarkable doubt of the authors cited above and repeated again here: 'Perhaps it is time to abandon the idea that a universal power law for non-dimensional fetch-limited growth rate is anything more than an idealization.'

Hwang & Wang (2004) and Hwang (2006) obtained the fetch-limited dependence 3.7 by means of conversion of one-point time series into dependence on fetch considering

the spatial growth as more physically relevant. Note, that such a conversion is heuristical rather than mathematically and physically well-founded.

When considering papers by Ross (1978), Liu & Ross (1980) (cases 3.8–3.10), our first idea was to put them into group 2 by the formal criteria – ‘true fetch-limited’ set-up. The airborne measurements were carried out in the Western Atlantic and North Sea (Ross 1978) and along a number of tracks in Michigan Lake (Liu & Ross 1980). Group 3 of ‘bad dependencies’ has been found more relevant after our attempts to find an explanation for the striking deviations of exponents p_χ , q_χ from theoretical dependence (2.38). The first dependence 3.8 (Ross 1978) was most probably affected by inaccuracies in measurements of wind along the aircraft tracks and scaling of data by instantaneous wind speed. Liu & Ross (1980) accepted this ocean wave-growth dependence without any criticism and used it as the predetermined one for the case of Lake Michigan where conditions of wind-wave interaction were probably (and, we believe, they certainly were) different from those in the Atlantic and North Sea. The authors tried to justify their data points not being inconsistent with some predetermined dependencies rather than attempting to produce a best statistical fit to those points. Their figures 4 and 5 with points for the stable stratification are reproduced here as our figure 10. Our best fit to the data is shown in this figure. This fit ($p_\chi = 0.52$, $q_\chi = 0.08$) is very different to that proposed by Liu & Ross ($p_\chi = 1.1$, $q_\chi = 0.27$), and our point would go completely off the scale in figure 9 of the present paper. The truth would be, apparently, somewhere in between if the Lake Michigan data were thoroughly statistically re-analysed. In table 2 we give our best fit as well.

The dependence 3.9 in Liu & Ross (1980) was obtained for unstable atmospheric conditions by a simple re-scaling of the wind speed within the logarithmic boundary-layer concept: only pre-exponents of wave-growth dependencies ε_0 , ω_0 were changed whereas previous exponents p_χ and q_χ were enforced (case 3.8).

Case 3.11 (Davidan 1996) gives maximal deviation from the theoretical dependencies, but is of special interest to us. This case can be considered as conceptually opposite to our approach. Davidan (1996) tried to scale different data sets by friction velocity u^* rather than by wind speed U_h at a reference height. Using the logarithmic wind speed profile as a model of the atmospheric boundary layer, he re-derived the wave-growth law for the new scaling for a number of data sets including JONSWAP. Thus, he linked implicitly *universality of wave growth* to universality and the *leading role of wave-wind interaction*. Alternatively, the asymptotic split balance model we used here to derive weakly nonlinear growth law (1.9) results from the *leading role of nonlinear wave-wave interactions*.

4.2.4. Group 4. Effect of wave tank data

Laboratory data are inapplicable to our theory, as was stressed above. This is why we finalize our list by two classical works on the problem of wave growth (Hasselmann *et al.* 1973; Mitsuyasu *et al.* 1971) which do include such data.

The kinetic description of water waves becomes invalid at typical rather short scales of wave development in wave tanks comprising at very best a few hundred wave periods. Therefore, wave tank data are completely irrelevant to our model of wind-wave sea. The use of laboratory data will corrupt the resulting dependencies in an unpredictable way. In the cited papers (Hasselmann *et al.* 1973; Mitsuyasu *et al.* 1971) these data seem to have corrupted the peak frequency dependence more than they did the energy dependence. Once Davidan (1980) and Phillips (1985) removed the laboratory data, the value of q_χ changed from 0.33 down to 0.28 and 0.25 whereas the value of p_χ stayed unchanged.

A number of other data points in our graphs (i.e. Mitsuyasu *et al.* 1971; Kahma 1981) reside precisely or almost precisely at the same location as the JONSWAP point (Hasselmann *et al.* 1973). It would be fair to mention that, although widely used dependencies with $p_\chi = 1$ and $q_\chi = 1/3$ are routinely attributed to the JONSWAP results, it was Mitsuyasu *et al.* (1971) who first obtained them. Therefore, it is possible that the need to attach the laboratory data to the field measurements of JONSWAP was brought about by a desire to conform with the Mitsuyasu *et al.* (1971) results; and dependencies of Mitsuyasu *et al.* (1971, 1982), just like the dependencies of JONSWAP, were based on a composite data set which included both the field and laboratory data. Besides, the field data of Hakata Bay (Mitsuyasu *et al.* 1971) belonged to quite short fetches, all below 8 km, and, thus, the relatively narrow range of fetch would give an additional support to the bias owing to the inclusion of the wave tank data.

Finalizing this analysis of the four groups of data points, we should emphasize the difficulty of sorting available wave-growth dependencies by formal criteria. Sometimes, dependencies relied upon in composite data sets show better conformance with theory than ‘true fetch-limited’ ones (e.g. 2.1 by Dobson *et al.* 1989), sometimes we have to move ‘true fetch-limited’ dependencies to the end of the list (e.g. Liu & Ross 1980) owing to suspicious data processing. We need an additional step – analysis of wave growth pre-exponents to make our sorting of the dependencies consistent.

4.3. Pre-exponents of fetch-limited wind-wave growth

Figure 11 shows the parameter of self-similarity α_{ss} as a function of p_χ estimated in accordance with (4.1). The range of ‘legitimate’ changes of the parameter α_{ss} for ‘the cleanest’ group 1 is from 0.3 to 0.65 (figure 11a). We should point out that this range should not be treated as a statistical scatter only around some universal value. Different values of α_{ss} are possible because it is a function of the rate p_χ , as was mentioned in the previous sections. Magnitudes of α_{ss} for groups 1 and 2 appear to be surprisingly close to that for the duration-limited case (see § 3.3. and figure 7). The proximity of duration- and fetch-limited estimates of the self-similarity parameter α_{ss} confirms (maybe somewhat indirectly) the general nature of the weakly turbulent relationship (1.9): the link of wave energy to the flux (total net input) does not depend on the wave-growth set-up. In the absence of numerical results for the fetch-limited wave development, this agreement of the estimates is of special value. This means that results of the duration-limited simulation can, with some caution, be applied to fetch-limited conditions for which such simulations are not available. Note that, strictly speaking, self-similarity parameters α_{ss} in duration- and fetch-limited cases are not identical in terms of relationships ((2.21), (2.43)) that imply particular scaling of characteristic frequency ω_* .

The consistent estimates of α_{ss} in groups 1 and 2 of our collection look remarkable and can be considered as a recognition of high quality of experimental measurements of wave growth. Equation (4.1) contains the pre-exponent of power fit in high power $\tilde{\omega}_0^{10/3}$ that makes estimates of α_{ss} very sensitive to errors of power-law fit. The pre-exponent $\tilde{\omega}_0$ in table 2 varies by factor 1.5 and its counterpart $\tilde{\epsilon}_0$ by 6.8.

Subsets of the JONSWAP experiment (cases 2.3 and 2.4) provide maximal outliers that can probably be explained by the effect of composite data sets. α_{ss} for the full JONSWAP data set (case 4.1, figure 11d) is significantly greater if compared to these subsets. Obviously, this is an effect brought about by the laboratory data.

Group 3 shows a strong scatter of estimates of α_{ss} . Maximal values of α_{ss} are found in cases 3.4–3.6 where the wave growth exponent p_χ was most probably

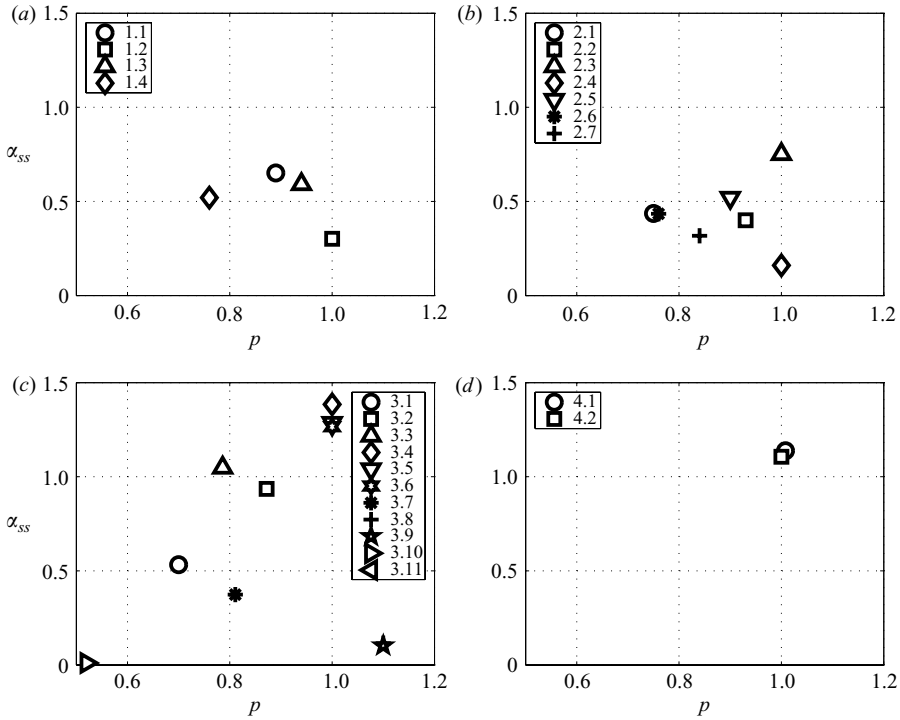


FIGURE 11. Dependence of α_{ss} on p_χ for fetch-limited experiments.

pre-determined by ‘reference figures’ of JONSWAP (Hasselmann *et al.* 1973). The errors in pre-determined exponents p_χ are not important by themselves (power $-1/3$ in (4.1)), but this constraint leads to errors of pre-exponents ε_0, ω_0 that enter the formula for α_{ss} to high powers. Similar enforcement of p_χ in cases 3.9–3.10 gives anomalously low values of α_{ss} .

Case 3.11 by Davidan (1996) requires a special comment: the estimate of $\alpha_{ss} = 3.74$ is beyond the limits of figure 11 (see table 3). As expected, the alternative scaling by Davidan (1996), which was fully re-normalized in terms of friction velocity, appears to be completely incomparable with the rest of 23 the dependencies if considered in terms of our weakly turbulent relationship (1.9). Thus, the idea of Davidan (1996) itself on universal scaling of wave growth by instantaneous friction velocity u^* (and, hence, on a leading wind-wave interaction) is not consistent with our approach based on the hypothesis of dominating wave-wave coupling.

5. Discussion

5.1. Toba law as a particular case of the weakly turbulent wind-wave growth law

It should be noted that it is, in fact, the first time that ‘the laws of wind-wave growth’ (as it is written in the paper title) are proposed in the sense that specific mechanisms of the growth are identified and described in terms of adequate physical quantities. Multiple mechanisms and the complexity of air–sea interaction lead workers to focus on cumbersome models of wind-wave growth rather than on the compact physics of wind-wave development. The only attempt to derive ‘a true physical law’ was by Toba (1972, 1793*a, b*).

The 3/2 Toba's law was derived from 'the local balance' of weakly nonlinear Stokes drift of water particles and wind stress. The Hasselmann kinetic equation and the associated nonlinear transfer escaped Toba's attention completely. Nevertheless, the conclusions showed a fairly good agreement with observations. Moreover, it can be shown that the Toba law can be considered, formally, as a particular case of the weakly turbulent law.

Assuming the net input $d\varepsilon/dt$ be constant, we immediately obtain the 3/2 law from (1.9): Toba law corresponds to the stationary energy input through wave development. Let us take Toba law in the following form (Toba 1997):

$$H_s = B(gu_*^3)^{1/2} T_s^{3/2},$$

where subscript s for period and height means 'significant', and $B = 0.062$. Converting significant wave height and wave period into the conventional energy and peak frequency, we have

$$\frac{\varepsilon \omega_p^4}{g^2} = \left(\frac{\pi^9 B^6 u_*^3 \omega_p^3}{g g^2} \right)^{1/3}.$$

Comparing with our law (1.9), we can obtain the rate of total energy accumulated by waves

$$\frac{d\varepsilon}{dt} = \frac{\pi^9 B^6 u_*^3}{g} = 0.0017 \frac{u_*^3}{g}.$$

Evident substitution should be made, taking into account the relative weakness of wind-wave interactions due to the differences of air and water densities

$$\frac{d\varepsilon}{dt} = 1.3 \frac{\rho_{air}}{\rho_{water}} \frac{u_*^3}{g}. \quad (5.1)$$

The estimate looks reasonable. Recent estimates of flux $d\varepsilon/dt$ based on a thorough study of the extensive data collection (Resio, Long & Vincent 2004) are consistent with (5.1) quantitatively.

Within the presented approach we are not able (have no right, in fact) to relate wave growth with characteristics of atmosphere (e.g. u^*). Within the split wave balance, we operate with the fluxes of energy (action, momentum) accumulated by the waves, but not with those coming from the wind (i.e. wind input minus dissipation). The physical mechanisms responsible for these fluxes are subjects of 'advanced theories' that take into account details of wind-sea interactions. We made just a first approximation that shows the importance of intrinsic nonlinear wave evolution for wind-wave growth. Alternative approaches (Toba's is a representative example of this kind) skip this step, focusing on coupling of waves and atmosphere and, thus, belittling, unintentionally, inherent features of nonlinear evolution of water waves.

Significance of the interpretation of the Toba law in terms of the present theory, however, extends far beyond an interesting academic exercise. Since the fetch-limited development commonly exhibits $p_\chi \approx 1$ (see table 2), i.e. approximately constant energy flux, friction velocity u_* can be used to estimate this flux in such special circumstances according to (5.1). We must stress here that it is not true in the general case: exponents $p_\tau \approx 3/2$ were observed in the Norwegian Sea (Sanders 1976; Janssen, Komen & Voogt 1984) that correspond to energy flux growing with time as \sqrt{t} . In some experimental records in the Black Sea (Babanin & Soloviev 1998b), this

anomalously steep wave growth has been observed as well. These cases will be studied in a separate paper.

5.2. Equilibrium range balance of wind-driven waves by Resio et al. (2004)

Within the split-wave balance concept, we operate with the fluxes of energy (action, momentum) accumulated by the waves, but not with those coming from the wind (i.e. wind input minus dissipation). In this way, we split, in fact, an intrinsic dynamics of waves and dynamics of air–sea interaction. A consistent development of our approach, thus, implies a specific ‘flux language’ to fit the wave-wave and wind-wave interactions. An important step in this direction has been made by Resio *et al.* (2004).

Resio *et al.* (2004) related spectral fluxes in the equilibrium range of wind-wave spectra (the frequency range of quasi-constant fluxes) to ‘an effective, or net, wind input’. The proposed parameterization of the net input (equation 19 in Resio *et al.* 2004) is consistent with Toba’s estimates (5.1) and allows us to estimate the total energy from our weakly turbulent law (1.9),

$$\frac{\varepsilon\omega_p^4}{g^2} = \alpha_{ss}\alpha_4 C_{nl}^{1/3} \frac{u_{10} - u_0}{2C_p}, \quad (5.2)$$

where $C_p = g/\omega_p$ – phase speed of spectral peak waves. In accordance with Resio *et al.* (2004) $C_{nl} = 0.4$ and $\alpha_4 = 0.006$ (see table 2 for u_{10} scaling). Accepting the estimate of $\alpha_{ss} = 0.5$ for the self-similarity parameter, we have

$$\frac{\varepsilon\omega_p^4}{g^2} = 0.0011 \frac{u_{10} - u_0}{C_p}, \quad (5.3)$$

which is very close to the JONSWAP parameterization of wind-wave energy (e.g. Hasselmann *et al.* 1973; Babanin & Soloviev 1998*a*). Thus, our approach extends results by Resio *et al.* (2004): rigid links of spectra and spectral fluxes in an equilibrium domain appear to be valid for a whole wind-wave range owing to self-similarity and quasi-universality of wind-wave spectra.

6. Conclusions

We finalize this paper by summarizing our results.

(i) First of all, the key theoretical result should be emphasized: evolution of growing waves is asymptotically governed by the weakly turbulent law (1.9). This law dictates dependence of the wave energy on spectral flux (total net input). The basic physical constant α_{ss}^* in (1.9) is a direct analogue of the Kolmogorov constants in the theory of weak turbulence (Zakharov & Filonenko 1966; Zakharov & Zaslavsky 1982; Zakharov *et al.* 1992). Note that the weakly turbulent law (1.9) does not depend on such features of wave development as duration- or fetch-limited set-up: estimates of the self-similarity parameter α_{ss} from numerical experiments and from experimental dependencies for duration- and fetch-limited cases gave remarkably close values.

(ii) The theory was verified by means of field experiment data. Available integral fetch-limited dependencies (23 cases) were re-analysed and related to the weakly turbulent self-similar relationships (1.9), (2.10), (2.38). Those corresponding to the self-similar development were identified on the basis of physics, data quality and initial data processing procedures. We should stress that we did not rely on theoretical results when sorting out the dependencies as ‘good’ or ‘bad’.

(a) First, the wave tank data, compared to the field data, should be related to a completely different physics which cannot be described by the kinetic

Hasselmann equation. Corresponding dependencies (e.g. Mitsuyasu *et al.* 1971, 1982; Hasselmann *et al.* 1973) based on ‘composite’ data sets should be excluded from further analysis unconditionally.

(b) Secondly, dependencies comprising spurious correlations of data owing to inadequate wind speed scaling or one-point measurements, as well as dependencies based on ‘noisy’ composite data sets corresponding to different rates of wave growth, should be filtered out as well.

‘True’ experimental exponents $p_{\tau(\chi)}$, $q_{\tau(\chi)}$ are found to satisfy theoretical relationships quite well. Energy growth exponent $p_{\tau(\chi)}$ exhibits a small positive bias if compared with the theoretical dependence both in duration- and fetch-limited cases. This is explained by the effect of a growing non-self-similar wave background that broadens the spectra. Experimentally, this broadening is observed as an integral spectral feature. Numerical experiments allow us to relate this effect to a periphery of wave spectra. In contrast to the ‘traditional’ vision of universality of exponents $p_{\tau(\chi)}$, $q_{\tau(\chi)}$, they can vary in a wide range, demonstrating a ‘flexibility’ of this aspect of wave growth.

(iii) The self-similarity parameter α_{ss} should be viewed, if compared with exponents $p_{\tau(\chi)}$, $q_{\tau(\chi)}$, as a more rigid feature of wave development: in spite of difficulties of estimating α_{ss} from experimental and numerical results (e.g. high powers of ω_0 in (3.4), (4.1)), it varies in a relatively narrow range which reflects the universality of the energy-flux relationship. Experimental estimates of α_{ss} were obtained for the first time. For stable or slowly growing wind speeds, at the moment we can recommend $\alpha_{ss} = 0.55 \pm 0.25$: more detailed estimates of this basic physical parameter is a subject of further study. It was confirmed that fetch-limited and time-limited values of α_{ss} are close, which is consistent with the basic concept of a weakly turbulent scenario: the concept of a rigid link between energy and energy flux.

Other results should be also listed here as important and useful consequences of the general weakly turbulent physics of wind-wave growth.

(a) A novel approach to the analysis of wind-wave data – method of energy-flux diagram – was proposed as an effective tool to identify the weakly turbulent stage of wind-wave evolution both qualitatively and quantitatively. Its efficiency was illustrated for results of numerical solutions of the Hasselmann equation. The capacity of the method for the analysis of a wider set of field experimental data and its consistency with conventional data-processing routines should be tested.

(b) Analysis of a particular case of constant energy input which corresponds to the Toba 3/2 law shows an important implication of our results for the wind-sea studies: the weakly turbulent relation of energy and flux allows us to determine the net flux coming to waves, based on knowledge of the wave energy. This is an extremely promising direction of wind-wave studies: fluxes in atmosphere can be estimated from an instantaneous state of growing wind sea.

The study refines and essentially extends the concept of universality of wind-wave growth as such: parameters of wave growth are not fixed values for some ‘ideal’ conditions, but depend on magnitudes and rates of fluxes of energy (wave action, momentum) to waves and, thus, can be predicted for a much broader range of conditions of growing wind-driven waves.

The research was conducted under the US Army Corps of Engineers W912HZ-04-P-0172, ONR N00014-06-C-0130, INTAS-8014, Russian Foundation for Basic Research N04-05-64784, 07-05-00648-a, 07-05-92211, ofi-a-05-05-08027 and Russian

Academy Program 'Mathematical methods of nonlinear dynamics'. This support is gratefully acknowledged.

REFERENCES

- ABDALLA, S. & CAVALERI, L. 2002 Effects of wind variability and variable air density on wave modeling. *J. Geophys. Res.* **107** (C7), doi:10.1029/2000JC000639.
- BABANIN, A. N. & SOLOVIEV, Y. P. 1998a Field investigation of transformation of the wind wave frequency spectrum with fetch and the stage of development. *J. Phys. Oceanogr.* **28**, 563–576.
- BABANIN, A. N. & SOLOVIEV, Y. P. 1998b Variability of directional spectra of wind-generated waves, studied by means of wave staff arrays. *Mar. Freshwater Res.* **49**, 89–101.
- BADULIN, S. I., PUSHKAREV, A. N., RESIO, D. & ZAKHAROV, V. E. 2005a Self-similar solutions of the Hasselmann equation and experimental scaling of wind-wave spectra. In *Frontiers of Nonlinear Physics. Proc. 2nd Intl Conf.* pp. 191–196.
- BADULIN, S. I., PUSHKAREV, A. N., RESIO, D. & ZAKHAROV, V. E. 2005b Self-similarity of wind-driven seas. *Nonlinear Proc. Geophys.* **12**, 891–946.
- BADULIN, S. I., BABANIN, A. V., PUSHKAREV, A. N., RESIO, D. & ZAKHAROV, V. E. 2006 Flux balance and self-similar laws of wind wave growth. In *9th International Workshop on Wave Hindcasting and Forecasting*. [Http://www.oceanweather.com/waveworkshop/9thWaves/Papers/Badulin.pdf](http://www.oceanweather.com/waveworkshop/9thWaves/Papers/Badulin.pdf).
- BELBEROV, Z. K., ZHURBAS, V. M., ZASLAVSKI, M. M. & LOBISHEVA, L. G. 1983 Integral characteristics of wind wave frequency spectra. In *Interaction of Atmosphere, Hydrosphere and Lithosphere in Near-Shore Zone of the Sea* (ed. Z. Belberov, V. Zakhariev, O. Kuznetsov, N. Pykhov, B. Filyushkin & M. Zaslavskii), pp. 143–154. Bulgarian Academy of Science Press (in Russian).
- CERC 1977 *Shore Protection Manual*, vol. 3. U S Army Coastal Engineering Research Center.
- DAVIDAN, I. N. 1980 Investigation of wave probability structure on field data. *Trudi GOIN* **151**, 8–26 (in Russian).
- DAVIDAN, I. N. 1995 *Problems of observations and mathematical modeling of wind waves*. St-Petersburg, Meteozdat (in Russian).
- DAVIDAN, I. N. 1996 New results in wind-wave studies. *Russian Met. Hydrol.* **4**, 42–49 (in Russian).
- DOBSON, F., PERRIE, W. & TOULANY, B. 1989 On the deep water fetch laws for wind-generated surface gravity waves. *Atmos. Ocean* **27**, 210–236.
- DONELAN, M. A. & PIERSON JR, W. J. 1987 Radar scattering and equilibrium ranges in wind-generated waves with application to scatterometry. *J. Geophys. Res.* **92** (C5), 4971–5029.
- DONELAN, M. A., HAMILTON, J. & HUI, W. H. 1985 Directional spectra of wind-generated waves. *Phil. Trans. R. Soc. Lond. A* **315**, 509–562.
- DONELAN, M., SKAFEL, M., GRABER, H., LIU, P., SCHWAB, D. & VENKATESH, S. 1992 On the growth rate of wind-generated waves. *Atmos. Ocean* **30**, 457–478.
- DONELAN, M. A., DOBSON, F. W., SMITH, S. D. & ANDERSON, R. J. 1993 On the dependence of sea surface roughness on wave development. *J. Phys. Oceanogr.* **23**, 2143–2149.
- DONELAN, M. A., BABANIN, A. V., YOUNG, I. R., BANNER, M. L. & MCCORMICK, C. 2005 Wave follower field measurements of the wind input spectral function. Part I. Measurements and calibrations. *J. Atmos. Ocean Technol.* **22**, 799–813.
- DONELAN, M. A., BABANIN, A. V., YOUNG, I. R. & BANNER, M. L. 2006 Wave-follower field measurements of the wind-input spectral function. Part II: Parameterization of the wind input. *J. Phys. Oceanogr.* **36**, 1672–1679.
- EFIMOV, V. V., KRIVINSKI, B. B. & SOLOVIEV, Y. P. 1986 Study of the energetic sea wind waves fetch dependence. *Meteorologiya i Gidrologiya* **11**, 68–75 (in Russian).
- EVANS, K. C. & KIBBLEWHITE, A. C. 1990 An examination of fetch-limited wave growth off the West coast of New Zealand by a comparison with the JONSWAP results. *J. Phys. Oceanogr.* **20**, 1278–1296.
- GEOGJAEV, V. V. & ZAKHAROV, V. E. 2007 Hasselmann equation revisited. In preparation.
- GODA, Y. 2003 Revisiting Wilson's formulas for simplified wind-wave prediction. *J. Waterway Port Coast. Ocean Engng* **129** (2), 93–95.
- HASSELMANN, K. 1962 On the nonlinear energy transfer in a gravity-wave spectrum. Part 1. General theory. *J. Fluid Mech.* **12**, 481–500.

- HASSELMANN, K. 1963a On the nonlinear energy transfer in a gravity-wave spectrum. Part 2. Conservation theorems; wave-particle analogy; irreversibility. *J. Fluid Mech.* **15**, 273–281.
- HASSELMANN, K. 1963b On the nonlinear energy transfer in a gravity-wave spectrum. Part 3. Evaluation of the energy flux and swell-sea interaction for a Neumann spectrum. *J. Fluid Mech.* **15**, 385–398.
- HASSELMANN, K., BARNETT, T. P., BOUWS, E., CARLSON, H., CARTWRIGHT, D. E., ENKE, K., EWING, J. A., GIENAPP, H., HASSELMANN, D. E., KRUSEMAN, P., MEERBURG, A., MULLER, P., OLBERS, D. J., RICHTER, K., SELL, W. & WALDEN, H. 1973 Measurements of wind-wave growth and swell decay during the Joint North Sea Wave Project (JONSWAP). *Deutsch. Hydrograph. Z. Suppl.* **12** (A8).
- HSIAO, S. V. & SHEMDIN, O. H. 1983 Measurements of wind velocity and pressure with a wave follower during MARSEN. *J. Geophys. Res.* **88** (C14), 9841–9849.
- HWANG, P. A. 2006 Duration and fetch-limited growth functions of wind-generated waves parameterized with three different scaling wind velocities. *J. Geophys. Res.* **111** (C02005), doi:10.1029/2005JC003180.
- HWANG, P. A. & WANG, D. W. 2004 Field measurements of duration-limited growth of wind-generated ocean surface waves at young stage of development. *J. Phys. Oceanogr.* **34**, 2316–2326.
- JANSSEN, P. A. E. M., KOMEN, G. J. & VOOGT, W. J. P. 1984 An operational coupled hybrid wave prediction model. *J. Geophys. Res.* **89**, 3635–3654.
- KAHMA, K. K. 1981 A study of the growth of the wave spectrum with fetch. *J. Phys. Oceanogr.* **11**, 1503–1515.
- KAHMA, K. K. 1986 On prediction of the fetch-limited wave spectrum in a steady wind. *Finn. Marine Res.* **253**, 52–78.
- KAHMA, K. K. & CALKOEN, C. J. 1992 Reconciling discrepancies in the observed growth of wind-generated waves. *J. Phys. Oceanogr.* **22**, 1389–1405.
- KAHMA, K. K. & PETERSSON, H. 1994 Wave growth in a narrow fetch geometry. *Global Atmos. Ocean Syst.* **2**, 253–263.
- KITAIGORODSKII, S. A. 1962 Applications of the theory of similarity to the analysis of wind-generated wave motion as a stochastic process. *Bull. Acad. Sci. USSR, Geophys. Ser. Engl. Transl.* **N1**, 105–117.
- KITAIGORODSKII, S. A. 1983 On the theory of the equilibrium range in the spectrum of wind-generated gravity waves. *J. Phys. Oceanogr.* **13**, 816–827.
- LAVRENOV, I., RESIO, D. & ZAKHAROV, V. 2002 Numerical simulation of weak turbulent Kolmogorov spectrum in water surface waves. In *7th Intl Workshop on Wave Hindcasting and Forecasting, Banff, October 2002*, pp. 104–116.
- LAVRENOV, I. V. 2003 *Wind Waves in Ocean. Physics and Numerical Simulation*. Springer.
- LIU, P. C. & ROSS, D. B. 1980 Airborne measurements of wave growth for stable and unstable atmospheres in lake Michigan. *J. Phys. Oceanogr.* **10**, 1842–1853.
- MITSUYASU, H., NAKAMURA, R. & KOMORI, T. 1971 Observations of the wind and waves in Hakata Bay. *Rep. Res. Inst. Appl. Mech. Kyushu University* **19**, 37–74.
- MITSUYASU, H., TASAI, H., SUHARA, F., MIZUNO, T., HONDA, S. O. T. & RIKIISHI, K. 1982 Observation of power spectrum of ocean waves using a clover-leaf buoy. *J. Phys. Oceanogr.* **10**, 286–296.
- PETERSSON, H. 2004 Wave growth in a narrow bay. PhD thesis, University of Helsinki, [ISBN 951-53-2589-7 (Paperback) ISBN 952-10-1767-8 (PDF)].
- PHILLIPS, O. M. 1977 *The Dynamics of the Upper Ocean*. Cambridge University Press.
- PHILLIPS, O. M. 1985 Spectral and statistical properties of the equilibrium range in wind-generated gravity waves. *J. Fluid Mech.* **156**, 505–531.
- PLANT, W. J. 1982 A relationship between wind stress and wave slope. *J. Geophys. Res.* **87** (C3), 1961–1967.
- PUSHKAREV, A. N., RESIO, D. & ZAKHAROV, V. E. 2003 Weak turbulent theory of the wind-generated gravity sea waves. *Physica D: Nonlin. Phenom.* **184**, 29–63.
- PUSHKAREV, A. N., RESIO, D. & ZAKHAROV, V. E. 2004 Second generation diffusion model of interacting gravity waves on the surface of deep water. *Nonlinear Proc. Geophys.* **11**, 329–342, sRef-ID: 1607-7946/npg/2004-11-329.
- RESIO, D. T., LONG, C. E. & VINCENT, C. L. 2004 Equilibrium-range constant in wind-generated wave spectra. *J. Geophys. Res.* **109** (C01018), doi:10.1029/2003JC001788.

- ROSS, D. B. 1978 On the use of aircraft in the observation of one- and two-dimensional ocean wave spectra. In *Ocean Wave Climate* (ed. M. D. Earle & A. Malahoff), pp. 253–267. Plenum.
- SANDERS, J. W. 1976 A growth-stage scaling model for the wind-driven sea. *Ocean Dyn.* **29**, 136–161.
- SNYDER, R. L., DOBSON, F. W., ELLIOT, J. A. & LONG, R. B. 1981 Array measurements of atmospheric pressure fluctuations above surface gravity waves. *J. Fluid Mech.* **102**, 1–59.
- STEWART, R. W. 1974 The air–sea momentum exchange. *Boundary-Layer Met.* **6**, 151–167.
- TOBA, Y. 1972 Local balance in the air–sea boundary processes. I. On the growth process of wind waves. *J. Oceanogr. Soc. Japan* **28**, 109–121.
- TOBA, Y. 1973a Local balance in the air–sea boundary processes. II. Partition of wind stress to waves and current. *J. Oceanogr. Soc. Japan* **29**, 70–75.
- TOBA, Y. 1973b Local balance in the air–sea boundary processes. III. On the spectrum of wind waves. *J. Oceanogr. Soc. Japan* **29**, 209–220.
- TOBA, Y. 1997 Wind-wave strong wave interactions and quasi-local equilibrium between wind and wind sea with the friction velocity proportionality. In *Nonlinear Ocean Waves* (ed. W. Perrie), *Advances in Fluid Mechanics*, vol. 17, pp. 1–59. Computational Mechanics.
- WALSH, E. J., HANCOCK III, D. W., HINES, D. E., SWIFT, R. N. & SCOTT, J. F. 1989 An observation of the directional wave spectrum evolution from shoreline to fully developed. *J. Phys. Oceanogr.* **19**, 1288–1295.
- WEBB, D. J. 1978 Non-linear transfers between sea waves. *Deep-Sea Res.* **25**, 279–298.
- WEN, S. C., ZHANG, D., PEIFANG, G. & BOHAI, C. 1989 Parameters in wind-wave frequency spectra and their bearings on spectrum forms and growth. *Acta Oceanol. Sin.* **8**, 15–39.
- WEN, S.-C., GUO, P.-F., ZHANG, D.-C., GUAN, C.-L. & ZHAN, H.-G. 1993 Analytically derived wind-wave directional spectrum. Part 2. Characteristics, comparison and verification of spectrum. *J. Oceanogr.* **49** (2), 149–172.
- YOUNG, I. R. 1999 *Wind Generated Ocean Waves*. Elsevier.
- ZAKHAROV, V. E. 1966 Problems of the theory of nonlinear surface waves. PhD thesis, Budker Institute for Nuclear Physics, Novosibirsk, USSR (in Russian).
- ZAKHAROV, V. E. 1992 Direct and inverse cascade in wind-driven sea and wave breaking. In *Proc. IUTAM Meeting on Wave Breaking (Sydney, 1991)* (ed. M. L. Banner & R. Grimshaw), pp. 69–91. Springer.
- ZAKHAROV, V. E. 1999 Statistical theory of gravity and capillary waves on the surface of a finite-depth fluid. *Eur. J. Mech. B/Fluids* **18**, 327–344.
- ZAKHAROV, V. E. 2005a Direct and inverse cascades in the wind-driven sea. In *AGU Geophys. Monograph*, pp. 1–9. Miami.
- ZAKHAROV, V. E. 2005b Theoretical interpretation of fetch limited wind-driven sea observations. *Nonlinear Proc. Geophys.* **12**, 1011–1020.
- ZAKHAROV, V. E. & FILONENKO, N. N. 1966 Energy spectrum for stochastic oscillations of the surface of a fluid. *Sov. Phys. Dokl.* **160**, 1292–1295.
- ZAKHAROV, V. E. & PUSHKAREV, A. N. 1999 Diffusion model of interacting gravity waves on the surface of deep fluid. *Nonlinear Proc. Geophys.* **6**, 1–10.
- ZAKHAROV, V. E. & ZASLAVSKY, M. M. 1982 The kinetic equation and Kolmogorov spectra in the weak-turbulence theory of wind waves. *Izv. Atmos. Ocean. Phys.* **18**, 747–753.
- ZAKHAROV, V. E. & ZASLAVSKY, M. M. 1983 Dependence of wave parameters on the wind velocity, duration of its action and fetch in the weak-turbulence theory of water waves. *Izv. Atmos. Ocean. Phys.* **19**, 300–306.
- ZAKHAROV, V. E., FALKOVICH, G. & LVOV, V. 1992 *Kolmogorov Spectra of Turbulence. Part 1*. Springer.